Inorganic Chemistry

Article

pubs.acs.org/IC

Low-Dimensional 3d–4f Complexes Assembled by Low-Spin $[Fe^{III}(phen)(CN)_4]^-$ Anions

Diana Visinescu,*[,†] Luminita Marilena Toma,[‡] Oscar Fabelo,[∥,⊥] Catalina Ruiz-Pérez,[§] Francesc Lloret,[‡] and Miguel Julve*[,‡]

[†]Coordination and Supramolecular Chemistry Laboratory, Institute of Physical Chemistry "Ilie Murgulescu", Romanian Academy, Splaiul Independentei 202, 060021 Bucharest, Romania

[‡]Departament de Química Inorgánica/Instituto de Ciencia Molecular, Facultat de Química de la Universitat de València, C/Catedrático José Beltrán 2, 46980 Paterna, Valencia, Spain

[§]Laboratorio de Rayos X y Materiales Moleculares, Departamento de Física Fundamental II, Facultad de Física de la Universidad de La Laguna, Avda. Astrofísico Francisco Sanchez s/n, 38204 La Laguna, Tenerife, Spain

[∥]Instituto de Ciencia de Materiales de Aragón, CSIC-Universidad de Zaragoza, Pedro Cerbuna 12, 50009 Zaragoza, Spain

[⊥]Institut Laue Langevin, B.P. 156, 6 Rue J. Horowitz, 38000 Grenoble, France

Supporting Information

ABSTRACT: The synthesis, crystal structure, and magnetic properties of four new mixed 3d–4f complexes with formulas $[\{Fe^{III}(phen)(CN)_4\}_4Gd_2^{III}(bpym)(NO_3)_2(H_2O)_4]\cdot 2CH_3CN\cdot 2H_2O\}_n$ (**1**), $[\{Fe^{III}(phen)(CN)_4\}_4Tb_2^{III}(bpym)(H_2O)_8]\cdot(NO_3)_2\cdot 2CH_3CN\}_n$ (**2**), $[\{Fe^{III}(phen)(CN)_4\}_4Sm^{III}(bpym)(NO_3)_2(H_2O)_5]\cdot 2CH_3CN\}_n$ (**3**), and $[\{Fe^{III}(phen)(CN)_4\}_2Pr_2^{III}(bpym)(NO_3)_4(H_2O)_2]_n$ (**4**) (phen = 1,10-phenanthroline and bpym = 2,2′-bipyrimidine) are discussed here. Compounds **1**–**3** are isomorphous and their structure consists of neutral ladder-like motifs where the rungs are made up by bpym-bridged dilanthanide(III) cations and the rods are defined by $[Fe(phen)(CN)_4]^-$ units adopting a bis-monodentate coordination mode through two of its four cyanide ligands. The electroneutrality in this family is achieved by either a chelating [at the Gd(III) (**1**) and Sm(III) (**3**)] or free [at the Tb(III) (**2**)] nitrate group and a peripheral $[Fe(phen)(CN)_4]^-$ entity, which act as a monodentate ligand across one of its four cyanide groups toward the rare-earth cation (**1**–**3**). Compound **4** exhibits a neutral two-dimensional structure where (μ-bpym)bis[diaquadi(nitrato-κ^2-*O*,*O*′)praseodymium(III)] fragments are interlinked through $[Fe(phen)(CN)_4]^-$ units adopting a tris-monodentate coordination mode across three of its four cyanide groups. Each iron(III) ion in **1**–**4** is six-coordinate with two nitrogen atoms from a chelating phen and four cyanide-carbon atoms building a somewhat distorted octahedral environment. The trivalent rare-earth cations are 9- (**1**–**3**) and 10-coordinate (**4**) having in common two nitrogen atoms from a bidentate bpym and three (**1**–**3**)/two (**4**) cyanide nitrogens, the coordination environment being completed by chelating nitrate (**1**, **3**, **4**) and water molecules (**1**–**4**). Magnetic susceptibility measurements in the 1.9–300 K temperature range show the occurrence of antiferromagnetic interactions in **1** through both the single cyanide- and the bis-bidentate bpym ligands. A weak ferromagnetic interaction is observed for **3** whereas very weak, if any, magnetic interactions would occur in **2** and **4**, with the spin–orbit coupling of the low-spin iron(III) ion and the ligand field effects of the Tb(III) (**2**) and Pr(III) (**4**) masking their visualization.

INTRODUCTION

Systems containing pairs of d–f type cations are very attractive for designing (multi)functional molecular materials. The richness of their structures and exciting magneto-optical properties justify the great interest in mixed transition-rare earth ions complexes.[1] An appealing case is represented by the cyanide-bridged heterospin $M^{III}(3d)$–Ln^{III} paramagnetic centers (M = Fe and Cr).[2] These systems are usually constructed from hexacyanometallate anions and Ln(III) cations, and they constitute good premises for interesting magnetic properties: (i) the increased connectivity of $[M^{III}(CN)_6]^{3-}$ (M = Cr and Fe) anions[3] combined with the high coordination numbers of the lanthanide(III) cations can lead to extended networks of the so-called hybrid Prussian Blue (PB) analogues. (ii) An efficient magnetic coupling mediated by the cyanide-bridge is expected between 3d and 4f orbitals. (iii) The large unquenched and/or anisotropic magnetic moments of the Ln(III) cations associated with the high-spin state/orbital contribution of the Cr(III)/Fe(III) transition metal ions create

Received: October 18, 2012
Published: January 18, 2013

   dx.doi.org/10.1021/ic302278q | *Inorg. Chem.* 2013, 52, 1525–1537

suitable conditions to achieve single molecule/chain magnets (SMMs/SCMs).[4]

A simple reaction between the negatively charged hexacyanoferrate(III) unit and lanthanide(III) cations gave rise to three-dimensional (3D) extended arrays of cyanide-bridged $Ln^{III}[Fe^{III}(CN)_6]\cdot 4H_2O$ (Ln = La, Pr, Nd, Sm, Gd, Dy, Er, and Y) systems, a few of them being magneto-structurally investigated.[5] Only two examples of such 3D systems, namely $Ln^{III}[Fe(CN)_6]\cdot 4H_2O$ (Ln = Sm and Tb), were molecular-based magnets[5e,f] which highlighted the importance of an increased dimensionality in the family of cyanide-bridged mixed 3d−4f complexes. The crystallization issues together with their highly symmetric face-centered cubic structure, with the lack or presence of a very low anisotropy, account for the reduced interest in such systems. Moreover, considering the large spin−orbit coupling of most of the Ln(III) cations, the f−d magnetic interaction is still far from being rationalized by means of empirical approaches, prompting the search for alternative hybrid PB systems.

One suitable strategy is the incorporation of a chelating organic ligand within the $Ln^{III}[M^{III}(CN)_6]$ lattice that would block some coordination sites of the lanthanide(III) cation[2,6−11] and also modify the solubility to make easier the growing of X-ray quality single-crystals. 2,2′-Bipyridine (bipy),[7a−e] 1,10-phenatroline (phen),[7f] 2,4,7,8-tetramethyl-1,10-phenantroline (tmphen), 2,4,6-tris(2-pyridyl)-1,3,5-triazine (tptz),[2e] and 2,2′:6′,2″-terpyridine (terpy)[2g] are illustrative examples of efficient nitrogen donor ligands which, in the complex formation processes between negatively charged hexacyanometallate units and rare-earth cations, have provided a straightforward preparative route of heterobimetallic chains.[7] A systematic study of some of these examples provided the first insights on the nature of the magnetic coupling between low-spin iron(III) and rare-earth cations across the cyanide bridge.[7b−d,f]

The structural peculiarities of the coligand as well as its number in the final formula strongly influence the network dimensionality and topology. When the divergent linear 4,4′-bipyridine-*N*,*N*′-dioxide (bpdo) was used (in excess) in the complex formation between Pr(III) cations and $[M(CN)_6]^{3-}$ (M = Fe and Co) anions, zigzag chains have been obtained.[8] A smaller amount of the bpdo ligand in a similar reaction with Ln(III) cations (Ln = Nd, Sm, Gd, and Tb) and hexacyanometallate(III) units extended the dimensionality to corrugated grid-like layered structures.[2b] Using a poliazine molecule, namely 2,2′-bipyrimidine (bpym), coordination to the Nd(III) cations as a bidentate ligand generated a 2D cyanide-bridged $M^{III}-Ln^{III}$ framework with fused rows of rhombuses.[9] Dimethylformamide (DMF) was intensively used as a terminal ligand in the reaction with lanthanide cations generating a rich family of dimers,[10] some of them exhibiting unusual photo(switched) magnetic properties.[2l,o,p,10e,f,k] Along with discrete species, 1D or 2D arrays with distinct topologies of cyanide-bridged $\{Fe^{III}Ln^{III}\}$ complexes were also obtained in DMF or monosulfoxide ligand-assisted reactions.[2c,d,f,k,m,11] Long-range magnetic ordering was observed for brick wall-like arrays when DMF was used as the auxiliary ligand.[11]

The use of heteroleptic metallocyanide precursors with a decreased number of cyanide groups is another possible option to gain some control on the dimensionality of the d−f assemblies. 4d and 5d cyanide-bearing complexes were successfully used in the complex formation with lanthanide(III) cations or $Ln^{III}-M^{II}$(3d) (M = Cu and Ni) preformed species to build low-dimensional systems with two or three distinct spin-carriers.[12,13] Cyanide-bearing $PPh_4[Fe(AA)(CN)_4]$ complexes (PPh_4^+ = tetraphenylphosphonium cation and AA = bipy and phen) were the first 3d heteroleptic precursors used as ligands toward lanthanide(III) cations in the presence of bpym.[14] They belong to a larger family of low-spin iron(III) tetracyanide-based precursors specially designed to limit the framework dimensionality, some of the synthesized hetero-bimetallic 1D assemblies being SCMs.[15,16] On the other hand, the free cyanide groups and the aromatic rings are known as noncovalent connectors (hydrogen-bonds and $\pi-\pi$ stacking interactions) leading to supramolecular frameworks.[14]

The bpym molecule has a rich chemical history as bidentate and bis-bidentate ligand toward *n*d (n = 3−5) metal ions[17−27] and more recently with rare-earth cations[12,28−32] or mixtures of 4d(5d) and lanthanide(III) centers.[33] The role of the polyazine ligand is expected to be multiple: improvement of the crystallization process, bridging capability, and structural directing agent as (supra)molecular connector. In the reaction between the six-coordinate $[Fe(bipy)(CN)_4]^-$ anions and lanthanide(III) cations, the introduction of bpym as a coligand partially blocks the coordination sphere of the Ln(III) ions acting as a bidentate ligand, and it also contributes to the stabilization of the supramolecular 3D networks through hydrogen bonds which run in conjunction with the $\pi-\pi$ stacking interactions between the aromatic rings of the bipy and/or bpym molecules.[14a] The reaction of the low-spin $[Fe(phen)(CN)_4]^-$ unit with lanthanide(III) cations and bpym, in a $CH_3CN:H_2O$ 1:1 (v/v) solution, afforded a series of hexanuclear compounds where two cyanide-bridged $\{Fe^{III}{}_2Ln^{III}\}$ heterobimetallic entities are linked by a bis-bidentate bpym molecule.[14b] This bis-chelating mode of the bpym molecule is quite common in its complexes with rare-earth cations.[28−32]

Herein we report the synthesis, structural description, and magnetic properties of a new series of isomorphous heterobimetallic cyanide- and bpym-bridged ladder-like chains of formula $[\{Fe^{III}(phen)(CN)_4\}_4Gd_2{}^{III}(bpym)(NO_3)_2(H_2O)_4]\cdot 2CH_3CN\cdot 2H_2O\}_n$ (**1**), $[\{Fe^{III}(phen)(CN)_4\}_4Tb_2{}^{III}(bpym)(H_2O)_8]\cdot(NO_3)_2\cdot 2CH_3CN\}_n$ (**2**), and $[\{Fe^{III}(phen)(CN)_4\}_4Sm_2{}^{III}(bpym)(NO_3)_2(H_2O)_5]\cdot 2CH_3CN\}_n$ (**3**). A second structural type, a 2D structure, the cyanide- and bpym-bridged praseodymium(III) derivative, namely $[\{Fe^{III}(phen)(CN)_4\}_2Pr_2{}^{III}(bpym)(NO_3)_4(H_2O)_2]_n$ (**4**), is also included.

EXPERIMENTAL SECTION

Materials. All the chemicals were purchased from commercial sources, and they were used as received. $PPh_4[Fe(phen)(CN)_4]\cdot 2H_2O$ was prepared as described in the literature.[16g] Elemental analyses (C, H, and N) were performed at the Centro de Microanálisis Elemental from the Universidad Complutense de Madrid. The values of the Fe:Ln molar ratio [2:1 for Ln = Gd (**1**), Tb (**2**), and Sm (**3**) and 1:1 for Ln = Pr (**4**)] were determined by electron probe X-ray microanalysis at the Servicio Interdepartamental of the University of Valencia.

Synthesis of the Compounds. Complexes **1**−**4** were obtained following the same general method: an acetonitrile solution (10 cm^3) of $PPh_4[Fe(phen)(CN)_4]\cdot 2H_2O$ (0.05 mmol) was poured into another acetonitrile solution (10 cm^3) containing bpym (0.05 mmol) and the corresponding lanthanide salt as $Ln(NO_3)_3\cdot 6H_2O$ (0.05 mmol) [Ln = Gd (**1**), Tb (**2**), Sm (**3**), and Pr(**4**)] (0.05 mmol). Slow evaporation of the solution at room temperature afforded red-

dx.doi.org/10.1021/ic302278q | *Inorg. Chem.* 2013, 52, 1525−1537

Table 1. Crystal Data and Details of Structure Determination for Compounds 1−4

	1	2	3	4
T (K)	293(2)	293(2)	293(2)	293(2)
formula	$C_{76}H_{50}Fe_4Gd_2N_{32}O_{12}$	$C_{76}H_{60}Fe_4Tb_2N_{32}O_{14}$	$C_{76}H_{54}Fe_4Sm_2N_{32}O_{11}$	$C_{40}H_{26}Fe_2Pr_2N_{20}O_{14}$
M	2141.38	2186.80	2115.62	1404.32
cryst syst	monoclinic	monoclinic	monoclinic	monoclinic
space group	$P2_1/c$	$P2_1/c$	$P2_1/c$	$P2_1/n$
a (Å)	7.5649(8)	7.6100(10)	7.6360(2)	9.6270(9)
b (Å)	15.708(3)	15.8000(10)	15.8490(3)	26.323(2)
c (Å)	34.689(5)	34.9370(10)	34.9820(9)	10.7260(9)
α (deg)	90.00	90.00	90.00	90.000(6)
β (deg)	94.689(9)	95.178(10)	94.9910(10)	113.844(6)
γ (deg)	90.00	90.00	90.00	90.000(7)
V (Å^3)	4108.3(10)	4183.6(6)	4217.57(17)	2486.1(4)
Z	2	2	2	2
index ranges	$-9 \le h \le 7$	$-9 \le h \le 10$	$-10 \le h \le 9$	$-12 \le h \le 8$
	$-20 \le k \le 18$	$-20 \le k \le 19$	$-20 \le k \le 18$	$-34 \le k \le 31$
	$-45 \le l \le 41$	$-40 \le l \le 45$	$-25 \le l \le 46$	$-13 \le l \le 13$
ρ_{calcd} (Mg m^{-3})	1.731	1.736	1.666	1.876
λ (Mo Kα, Å)	0.710 73	0.710 73	0.710 73	0.710 73
μ (Mo Kα, mm^{-1})	2.360	2.426	2.117	2.583
R1, $I > 2\sigma(I)$ (all)	0.0783 (0.1332)	0.0879 (0.1069)	0.0993(0.1154)	0.0458(0.0674)
wR2, $I > 2\sigma(I)$ (all)	0.1372 (0.1550)	0.2263(0.2441)	0.2698 (0.2853)	0.0684(0.0730)
measured reflns (R_{int})	21 016 (0.0492)	47 856 (0.1165)	17 431 (0.0466)	14 336(0.0328)
indep reflns [$I > 2\sigma(I)$]	8824 (5747)	9640(8024)	8445 (7347)	5395 (4294)
no. refined params (restraints)	569(5)	577(4)	605(9)	352(0)

brownish prisms of **1**−**4** after a few days. The yield is about 40%. Anal. Calcd for $C_{76}H_{50}Fe_4GdN_{32}O_{12}$ (**1**): C, 42.58; H, 2.33; N, 20.69. Found: C, 43.21; H, 2.42; N, 20.45%. Anal. Calcd for $C_{76}H_{60}Fe_4Tb_2N_{32}O_{14}$ (**2**): C, 41.7; H, 2.74; N, 20.48. Found: C, 42.35; H, 2.89; N, 20.54%. Anal. Calcd for $C_{76}H_{54}Fe_4Sm_2N_{32}O_{11}$ (**3**): C, 43.1; H, 2.55; N, 21.17. Found: C, 43.52; H, 2.70; N, 21.25%. Anal. Calcd for $C_{40}H_{26}Fe_2Pr_2N_{20}O_{14}$ (**4**): C, 34.18; H, 1.85; N, 19.93. Found: C, 35.6; H, 2.15; N, 19.98%. Main IR peaks (cm^{-1}): 3408(m), 2929(w), 2856(w), 2148 (s), 2120(w), 2071(m), 1640(m), 1585(m), 1560(m), 1385(s), 1295(m), 1151(m), 1037(m), 853(m), 719(m) (**1**); 3415(m), 2929(w), 2855(w), 2149(s), 2120(w), 2059(m), 1660(m), 1584(m), 1560(m), 1385(s), 1295(m), 1152(m), 1037(m), 853(m), 723 (m) (**2**); 3411(m), 2925(w), 2859(w), 2145(s), 2120 (w), 2067(m), 1666(m), 1582(m), 1570(m), 1499(m), 1384(m), 1290(s), 1032(m), 851(m), 722(m) (**3**); 3415(m), 2926(w), 2860(w), 2145(s), 2120 (w), 2067(m), 1665(m), 1581(m), 1570(m), 1499(m), 1384(s), 1299(s), 1029(m), 850(m), 723(m) (**4**).

Physical Measurements. The IR spectra of **1**−**4** were registered on a Bruker IF S55 spectrometer as KBr pellets in the 4000−400 cm^{-1} range. Magnetic susceptibility measurements on crushed crystals (mixed with grease to avoid the crystallite orientation) of **1**−**4** were carried out with a Quantum Design MPMSXL-5 SQUID magnetometer in the temperature range 1.9−300 K and under applied dc magnetic fields covering the range 100 G−1 T. The magnetization versus the magnetic field measurements were performed at 2.0 K in the field range 0−5 T. Diamagnetic corrections for the constituent atoms and also for the magnetization of the sample holder were done.

Crystallographic Data Collection and Structure Determination. Suitable single crystals of compounds **1**−**4** were mounted on a Bruker Nonius Kappa CCD diffractometer. Diffraction data for all compounds were collected at 293(2) K using graphite-monochromated Mo Kα radiation (λ = 0.710 73 Å). The orientation matrix and lattice parameters for **1**−**4** were obtained by least-squares refinement of the reflections obtained by a θ−χ scan (Dirax/lsq method). Data collection and data reduction for all compounds were done with the COLLECT[34] and EVALCCD[34b] programs. Numerical absorption corrections were carried out for all compounds using PLATON software.[35] All the measured independent reflections were used in the analysis.

The structure was solved by direct methods and refined with full-matrix least-squares technique on F^2 using the SHELXS-97 and SHELXL-97 programs[36] included in the WINGX software package.[37] All non-hydrogen atoms were refined anisotropically. The hydrogen atoms were set in geometrical positions and refined with a riding model. Some disorder was found involving the position of the nitrate ion in **3**: two different positions were refined, giving rise to two different models, one with the nitrate in the lanthanide coordination sphere and the other one with a free. The refinement of the occupancy factors for each model gives rise to values of 55% and 45% for coordinated and free nitrate ions, respectively. As a consequence, when the nitrate ion is noncoordinated, a water molecule [O(3w)] belongs to the environment of the lanthanide cations. Due to the low diffraction power of these samples as well as the disorder present in compound **3**, soft restraints have been used to fix planarity and bond distances within the nitrate ions for compounds **1**−**3**. The occurrence of these problems precludes an accurate crystal structure determination as evidenced by the relatively high values of the agreement parameters (see Table 1); however, such data allow the refinement of the crystal structures with a reasonably good description. A summary of the crystallographic data and structure refinement is given in Table 1. Selected bond lengths and angles as well as hydrogen bonds for **1**−**3** are listed in Tables 2 and 3, respectively, whereas main bond lengths and angles for **4** are grouped in Table 4. The final geometrical calculations and the graphical manipulations were carried out with PARST97[38] and DIAMOND[39] programs, respectively. Crystallographic information is deposited in the CCDC database with numbers 903519 (**1**), 903520 (**2**), 903521 (**3**), and 903522 (**4**).

RESULTS AND DISCUSSION

Synthesis and Infrared Spectra. The 4f cations are very sensitive to any subtle change of their environment. In DMF or monosulfoxide ligand-assisted reactions, it has been observed that higher-dimensional PB analogues (chains or 2D arrays) were obtained either by working in anhydrous reaction conditions[2d,k,11] or by controlling the reactants/solvent molar

dx.doi.org/10.1021/ic302278q | Inorg. Chem. 2013, 52, 1525−1537

Table 2. Bond Lengths (Å) and Angles (deg) of the Coordination Environments of Fe(III) and Ln(III) in 1−3 [Ln(III) = Gd(III) (1), Tb(III) (2), and Sm(III) (3)][a]

	1	2	3
Ln(1)−O(1W)	2.387(8)	2.402(10)	2.444(13)
Ln(1)−O(2W)	2.404(9)	2.408(11)	2.442(14)
Ln(1)−O(3W)		2.387(19)	2.46(3)
Ln(1)−O(4W)		2.519(8)	
Ln(1)−O(1A)	2.350(12)		2.44(2)
Ln(1)−O(2A)	2.505(7)		2.563(11)
Ln(1)−N(1)	2.484(7)	2.476(9)	2.522(10)
Ln(1)−N(3)[(b)]	2.527(8)	2.547(11)	2.588(14)
Ln(1)−N(5)	2.456(7)	2.469(10)	2.517(10)
Ln(1)−N(13)	2.651(8)	2.651(8)	2.694(10)
Ln(1)−N(14)[(a)]	2.635(7)	2.661(8)	2.680(9)
Fe(1)−C(1)	1.917(7)	1.900(10)	1.912(13)
Fe(1)−C(2)	1.930(11)	1.958(14)	1.954(16)
Fe(1)−C(3)	1.931(10)	1.956(11)	1.964(13)
Fe(1)−C(4)	1.939(10)	1.953(10)	1.955(14)
Fe(1)−N(9)	1.984(8)	1.975(11)	1.982(13)
Fe(1)−N(10)	2.000(7)	1.996(10)	2.009(10)
Fe(2)−C(5)	1.887(9)	1.902(10)	1.887(13)
Fe(2)−C(6)	1.909(12)	1.939(14)	1.960(17)
Fe(2)−C(7)	1.920(11)	1.960(14)	1.942(17)
Fe(2)−C(8)	1.918(12)	1.960(13)	1.963(16)
Fe(2)−N(11)	1.990(7)	1.992(8)	1.996(10)
Fe(2)−N(12)	2.010(7)	2.029(9)	2.036(11)
Fe(1)−C(1)−N(1)	173.6(8)	172.9(9)	172.6(12)
Fe(1)−C(2)−N(2)	176.5(11)	174.4(13)	175.3(16)
Fe(1)−C(3)−N(3)	176.1(9)	175.5(10)	175.8(12)
Fe(1)−C(4)−N(4)	178.3(9)	178.0(10)	178.0(13)
Fe(2)−C(5)−N(5)	175.2(8)	175.7(9)	176.7(14)
Fe(2)−C(6)−N(6)	175.5(12)	173.5(14)	175.1(18)
Fe(2)−C(7)−N(7)	173.9(11)	175.6(14)	174.8(17)
Fe(2)−C(8)−N(8)	179.1(11)	178.4(13)	178.3(16)
Ln(1)−C(1)−N(1)	172.4(7)	172.6(8)	171.3(10)
Ln(1)−C(3)−N(3)	151.1(7)	151.7(9)	151.1(11)
Ln(1)−C(5)−N(5)	159.8(8)	160.3(9)	158.7(12)
N(9)−Fe(1)−N(10)	81.5(3)	81.7(3)	82.1(5)
N(11)−Fe(2)−N(12)	82.5(3)	82.8(3)	82.2(4)
N(13)−Ln(1)−N(14)[(a)]	60.8(2)	61.5(2)	60.6(3)
O(1A)−Ln(1)−O(2A)	61.0(4)		52.9(6)

[a]Symmetry code: (*a*) = 1 − *x*, 1 − *y*, -*z*; (*b*) = 1 + *x*, *y*, *z*.

Table 3. Selected Intermolecular Contacts (Å) in 1−3[a]

	1	2	3
O(1w)···N(2)[(d)]	2.780(13)	2.757(15)	2.762(20)
O(2w)···N(7)[(c)]	2.764(17)	2.753(18)	2.74(2)
O(2w)···O(3A)[(c)]	2.755(13)		2.85(3)
O(2w)···O(3B)[(c)]		2.795(18)	2.68(4)
O(3w)···O(1A)	2.71(3)		
O(3w)···O(3A)	2.23(2)		
O(3w)···O(1B)		2.66(3)	
O(3w)···O(2B)			2.76(3)
O(3w)···O(2B)[(e)]			2.67(4)
O(3w)···O(3B)		2.43(3)	
O(3w)···O(3A)[(f)]	3.15(3)		
O(4w)···O(3B)		2.424(18)	

[a]Symmetry code: (c) = −1 + *x*, *y*, *z*; (d) = −*x*, 1 − *y*, −*z*; (e) = 1 − *x*, 2 − *y*, −*z*; (f) = −1 + *x*, 2 − *y*, −*z*.

Table 4. Main Bond Lengths (Å) and Angles (deg) for 4[a]

Pr(1)−O(1W)	2.495(4)	Pr(1)−N(7)	2.720(4)
Pr(1)−O(1)	2.578(4)	Fe(1)−C(1)	1.926(5)
Pr(1)−O(2)	2.598(4)	Fe(1)−C(2)	1.917(6)
Pr(1)−O(4)	2.582(4)	Fe(1)−C(3)	1.935(5)
Pr(1)−O(5)	2.590(3)	Fe(1)−C(4)	1.951(5)
Pr(1)−N(1)	2.616(4)	Fe(1)−N(5)	1.988(4)
Pr(1)−N(3)[(c)]	2.584(5)	Fe(1)−N(6)	2.003(4)
Pr(1)−N(4)[(c)]	2.575(5)		
Fe(1)−C(1)−N(1)	175.8(4)	Pr(1)−N(1)−C(1)	167.1(4)
Fe(1)−C(2)−N(2)	176.6(5)	Pr(1)−N(3)−C(3)	143.0(4)
Fe(1)−C(3)−N(3)	177.4(4)	Pr(1)−N(4)−C(4)	153.0(4)
Fe(1)−C(4)−N(4)	178.0(5)	O(1)−Pr(1)−O(2)	48.51(13)
N(5)−Fe(1)−N(6)	82.13(18)	O(4)−Pr(1)−O(5)	48.84(12)
		N(7)−Pr(1)−N(8)[(a)]	59.44(11)

[a]Symmetry code: (a) = 2 − *x*, −*y*, 2 − *z*; (c) = 1 − *x*, −*y*, 2 − *z*.

ratio with a considerable decrease of the solvent amount (ball-milling method).[2c,f,m] In anhydrous acetonitrile and 1:1 acetonitrile/water mixture, the two supramolecular arrangements involving separated $[Fe^{III}(bipy)CN)_4]^-$ and $[Ln(bpym)(NO_3)_2(H_2O)_n]^+$ ion pairs are caused by the distinct coordination numbers and geometries of the lanthanide(III) cations with some interferences of their ionic radius.[14a] The lattice water molecules [8 (Eu, Tb, and Ho) and 11 (Gd)] in the series of cyanide- and bpym-bridged $\{Fe^{III}_2Ln^{III}\}_2$ complexes form hydrogen bonds with coordinated water molecules from the lanthanide(III) coordination sphere and terminal cyanide groups, interlinking the neutral hexanuclear entities into noncovalent 3D networks. Thus, it can be concluded that more anhydrous reaction conditions should lead to a reduction of the number of crystallization water molecules in the resulting 3d−4f systems and also to an increase of their dimensionality. Indeed, a similar reaction of the $[Fe(phen)(CN)_4]^-$ anion with trivalent rare-earth cations and bpym, which was carried out in a minimum amount of acetonitrile, afforded two extended structural types: a ladder-like motif [Ln = Gd (**1**), Tb (**2**), and Sm (**3**)] and a layered network [Ln = Pr (**4**)].

The infrared spectra of **1**−**4** are very similar, and we will focus mainly on the stretching vibrations of the bpym and cyanide ligands because of the possibility to infer their coordination modes. A sharp and splitted absorption at ca. 2145−2148 cm^{-1} is due to the bridging cyanide groups, while the lower-intensity frequencies located at ca. 2067 cm^{-1} are characteristic of the terminal cyanide ligands. The ring-stretching modes of coordinated bpym and phen ligands overlap in the 1640−1560 cm^{-1} region. The medium intensity bands at ca. 850 and 722 cm^{-1} are assigned to the chelating phen ligand. The strong absorptions at 1384−1388 cm^{-1} are due to the presence of the nitrate groups while the crystallization acetonitrile molecule in compounds **1**−**3** is clearly visible as a weak intensity peak at ca. 2300 cm^{-1} (stretching vibration of the C≡N bond). All these spectral features for **1**−**4** are in agreement with their crystal structures (see below).

Description of the Crystal Structures. *$[\{Fe^{III}(phen)(CN)_4\}_4Gd_2^{III}(bpym)(NO_3)_2(H_2O)_4]\cdot 2CH_3CN\cdot 2H_2O\}_n$ (**1**), $[\{Fe^{III}(phen)(CN)_4\}_4Tb_2^{III}(bpym)(H_2O)_8]\cdot(NO_3)_2\cdot 2CH_3CN\}_n$ (**2**), and $[\{Fe^{III}(phen)(CN)_4\}_4Sm_2^{III}(bpym)(NO_3)_2(H_2O)_5]\cdot 2CH_3CN\}_n$ (**3**).* Compounds **1**−**3** are isomorphous, and they crystallize in the monoclinic space group $P2_1/c$. The common structural

dx.doi.org/10.1021/ic302278q | Inorg. Chem. 2013, 52, 1525−1537

features of the **1**−**3** series of complexes are the development of the 1D double-chains exhibiting a ladder-like motif (Figure 1)

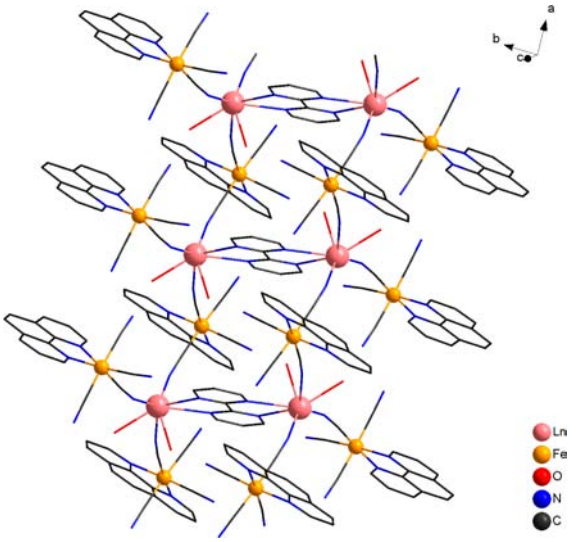

Figure 1. Perspective view of a fragment of the ladder-like motif in **1**−**3**.

and the presence of one free acetonitrile molecule. The ladders are built by zigzag rails consisting of repeating cyanide-linked $\{Fe^{III}{}_2Ln^{III}\}$ heterotrimetallic fragments which are connected by the bis-chelating bpym ligands acting as rungs (Supporting Information, Figure S1). Each $[Ln^{III}(NO_3)(H_2O)_x(bpym)]^{2+}$ unit interacts with two $[Fe(phen)(CN)_4]^-$ anions via single cyanide-bridges and also with a neighboring Ln(III) cation from the adjacent parallel chain, through the bpym ligand [x = 2 for 1, x = 4 for **2**, x = 2.5 for **3**]. The poliazine molecule bridges consecutively, following the a axis, two adjacent lanthanide(III) metal centers belonging to two different rods.

The ladder can be viewed also as assembled from intraconnected cyanide- and bpym-bridged $\{Fe_2^{III}Ln^{III}\}_2$ hexanuclear fragments whose structural characteristics are expected to be very similar to the previously reported oligonuclear $[\{Fe^{III}(phen)(CN)_3(\mu\text{-}CN)\}_4Ln_2^{III}(NO_3)_2(H_2O)_6(\mu\text{-bpym})]\cdot nH_2O$ [Ln = Eu, Dy, Ho, n = 8; Ln = Gd, n = 11] complexes.[14b] Each of the constituting $\{Fe_2^{III}Ln^{III}\}_2$ hexanuclear fragments in **1**−**3** lies on an inversion center located at (0.5, 0.5, 0) position in the plane of the bpym molecule.

The environment of the low-spin iron(III) cation is similar for all three compounds, and then, a common discussion of its main structural features will be carried out. The asymmetric unit in **1**−**3** is shown in Figure 2. Two crystallographically independent iron(III) metal centers [Fe(1) and Fe(2)] occur in **1**−**3**. They are six-coordinated in a distorted octahedral surrounding which is built by four cyanide groups and a bidentate phen molecule. The Fe−N and Fe−C bond lengths vary in the ranges 1.985(8)−2.010(8) (**1**), 1.978(10)−2.026(9) (**2**), and 1.982(13)−2.036(11) (**3**) Å (Fe−N), and 1.889(10)−1.939(10) (**1**), 1.904(11)−1.959(13) (**2**), and 1.887(13)−1.964(13) (**3**) Å (Fe−C), and they all agree with those observed for the related mononuclear species.[16g,h] The main source of the distortion of the octahedral polyhedron at the

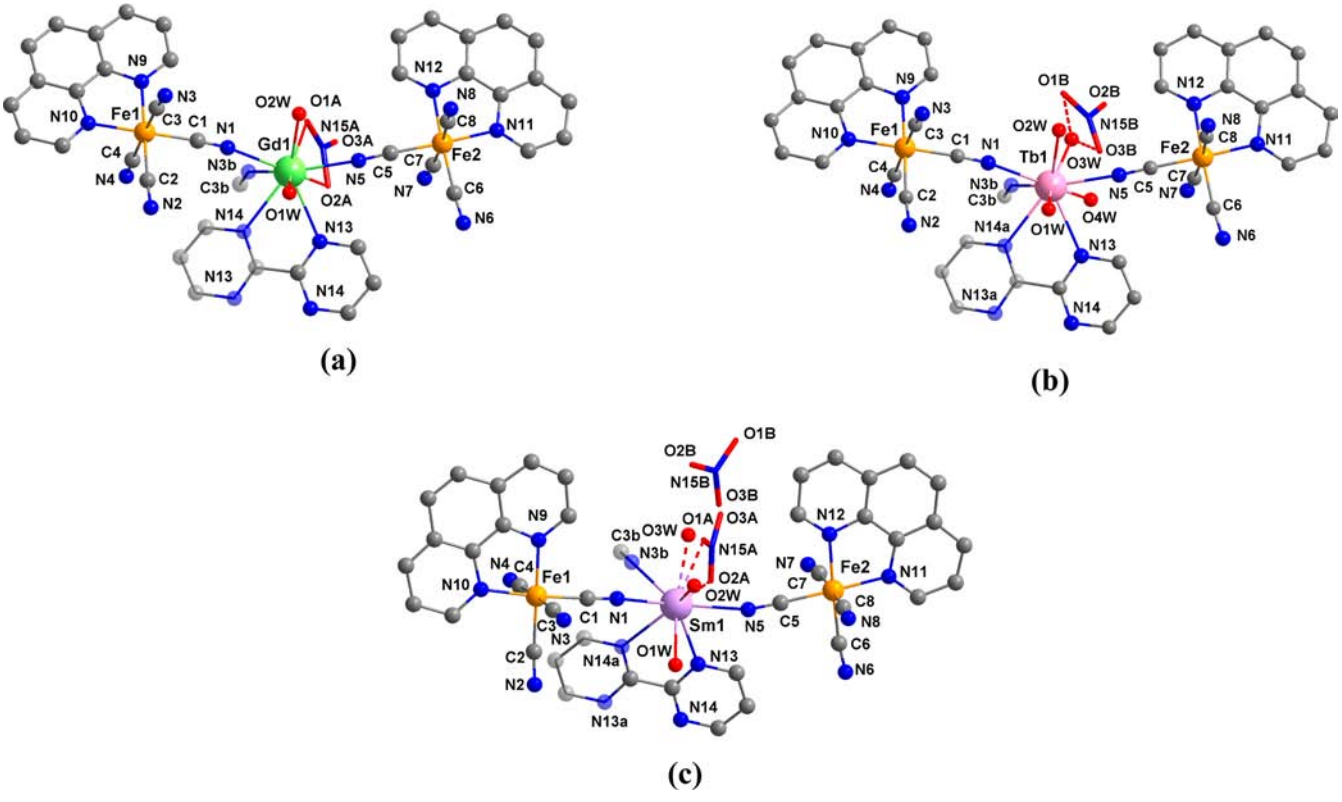

Figure 2. View of a fragment of **1** (a), **2** (b), and **3** (c) showing the most relevant atom numbering. The asymmetric unit has been represented in the sphere mode, with the exception of the nitrate group (disordered in the case of **3**), which has been drawn in the stick mode. The atoms generated by symmetry operations have been represented in the transparent mode. The hydrogen bonds in **2** are shown as dashed, whereas in **3**, they denote the possibility of the nitrate ion to be coordinate or free. Symmetry code: (a) = 1 − x, 1 − y, −z, (b) = 1 + x, y, z.

dx.doi.org/10.1021/ic302278q | Inorg. Chem. 2013, 52, 1525−1537

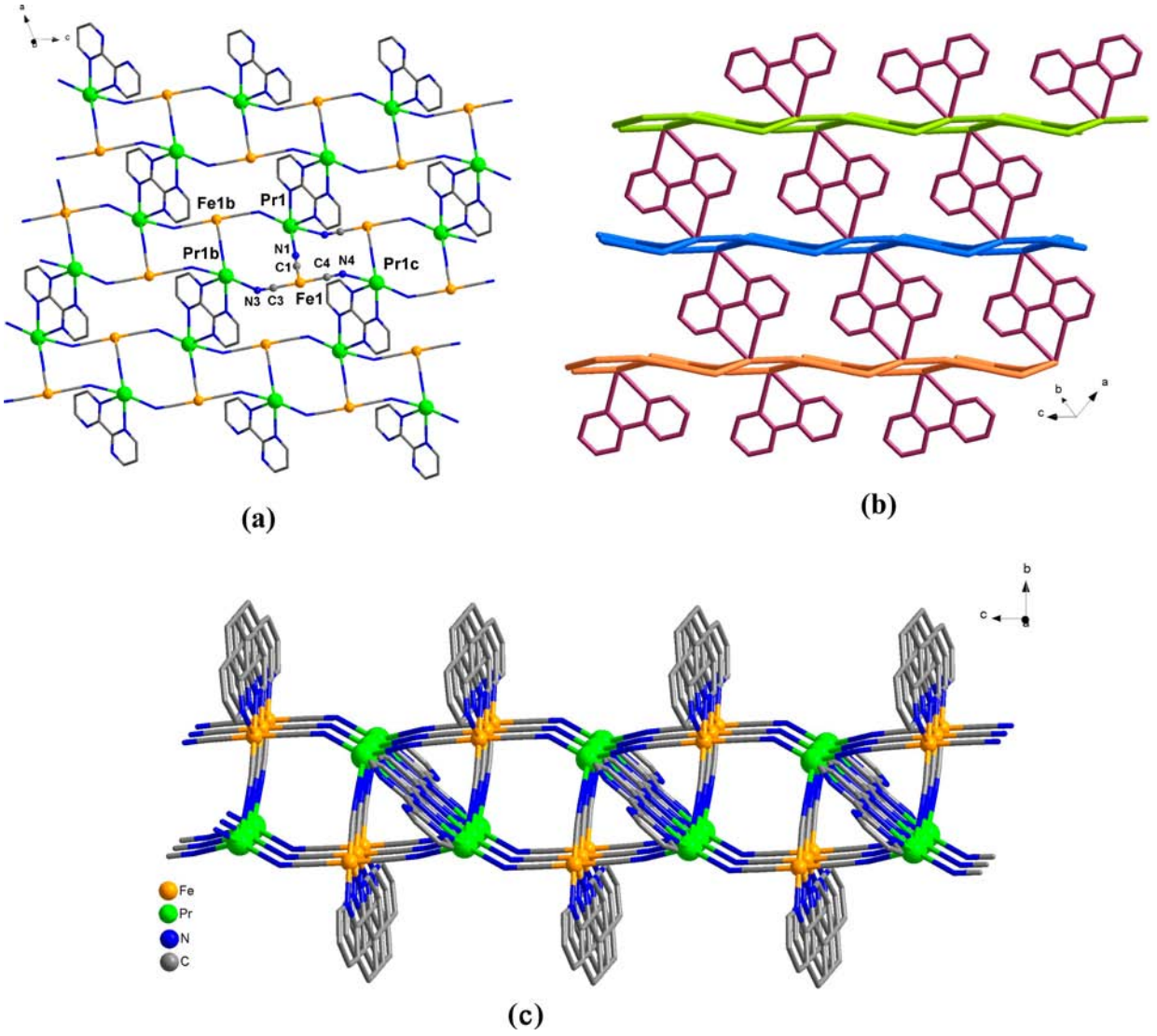

Figure 3. (a) View in the *ac* plane showing a fragment of the layer arising from the assembling of cyanide-based double-rods and bpym ligands. (b) Perspective view of the distinct corrugated double-chains (represented in orange, blue, and green) linked by the bpym molecules (drawn in violet). (c) Perspective view of the assembled bilayers extending in the *ac* plane [symmetry codes: (a) = 2 − *x*, −*y*, 2 − *z*; (b) = 1 − *x*, −*y*, 1 − *z*] (the terminal cyanide ligands, the water and nitrate groups, and the hydrogen atoms were omitted for clarity).

iron center is the short bite angle of the phenanthroline ligand [81.4(3)° (**1**), 81.6(4)° (**2**), and 82.1(5)° (**3**) at Fe(1), and 82.5(3)° (**1**), 82.7(4)° (**2**), and 82.2(4)° (**3**) at Fe(2)].

The Fe(1) and Fe(2) ions are linked to the Ln(1) cations in a different manner. The six-coordinated $[Fe(2)(phen)(CN)_4]$ moiety acts as a monodentate ligand toward the Ln(1) atom through one of its four cyanide groups, being the capping unit of one rod. The values of the intrachain Fe(2)···Ln(1) distance for **1**−**3** are quasi-identical [5.3871(16) (**1**), 5.3976(15) (**2**), and 5.4294(18) (**3**) Å]. The cyanide-bearing $\{Fe(1)(phen)(CN)_4\}$ fragment adopts a bis-monodentate coordination mode through two *cis*-cyanide groups toward two lanthanide cations belonging to the same rod. The values of the intrarod metal−metal separation are 5.4964(13) (**1**), 5.5051(15) (**2**), and 5.5398(17) (**3**) Å [Fe(1)···Ln(1) across C(1)−N(1)] and 5.3882(16) (**1**), 5.4315(15) (**2**), and 5.4611(18) (**3**) Å [Fe(1)···$Ln(1)^{(b)}$ through C(3)−N(3); (b) = −1 + *x*, *y*, *z*)]. One rod is developed following the crystallographic *a* axis, from repeating {Fe(1)−C(1)−N(1)−Ln(1)−N(3)−C(3)−Fe(2)} fragments which are connected to each other through the $Ln(1)^{(b)}$−N(3)−C(3) sequences. The Fe−$CN_{cyanide}$ set of atoms are close to linearity [173.6(8)−178.3(9)° (**1**), 172.9(9)−178.1(1)° (**2**), and 172.6(12)−178.0(18)° (**3**) at Fe(1), and 173.9(11)−179.9(11)° (**1**), 173.5(14)−178.4(16)° (**2**), and 174.8(17)−178.3(16)° (**3**) at Fe(2)], with the greater bending occurring at the cyanide bridges from the Fe(1) unit.

The Ln(1)−O bond lengths in **1**−**3** have values very close spanning the ranges 2.35(1)−2.505(7) (**1**), 2.386(12)−2.519(8) (**2**), and 2.443(12)−2.46(3) (**3**) Å (see Table 2). The largest distances are associated with the Ln(1)−N_{bpym} bonds [2.637(7) and 2.652(7) (**1**), 2.650(8) and 2.661(8) (**2**), 2.681(10)−2.695(10) (**3**) Å], and they represent the main source of the polyhedron distortion. The values of the Ln(1)−$N_{cyanide}$ bond lengths are 2.454(8) and 2.528(8) (**1**), 2.469(10) and 2.548(9) (**2**), and 2.517(11) and 2.522(10) (**3**) Å. The cyanide at the lanthanide side largely departs from linearity with values in the range 151.1(7)−172.4(7) (**1**)°, 151.7(9)−172.6(8)° (**2**), and 151.1(11)−171.3(10)° (**3**), the highest bend angles concerning the Ln(1)−N(3)−C(3) intrastrand connecting fragment.

dx.doi.org/10.1021/ic302278q | *Inorg. Chem.* 2013, 52, 1525−1537

The differences in the structures of compounds **1**−**3** are noticed in the lanthanide coordination sphere. So, the gadolinium(III) ion in **1** is nine-coordinate by five nitrogen atoms (three of the cyanide groups and two from bis-chelated bpym ligand) and four oxygen atoms (two water molecules and a bidentate nitrate anion) building a distorted monocapped square antiprism (Supporting Information, Figure S2a). The coordination number is also nine for the rare-earth cation in **2**, but the nitrate anions from the Gd(III) cation are replaced by two water molecules at the coordination sphere of the terbium(III) cation. The O(1W), O(4W), N(1), N(2), N(3), N(13), and N(14) set of atoms describes a distorted monocapped square antiprism polyhedron (Supporting Information, Figure S2b). The free nitrate anion in **2** is connected to the ladder-like motif through hydrogen bonds [O3W···O3B = 2.4273(34) and O1B···O3W = 2.6627(3) Å]. Unfortunately, the disordered nitrate groups in **3** preclude an accurate determination of the coordination sphere of samarium(III) cation (see Figure 3c). The lanthanide environment contains one chelated bpym ligand, three cyanide groups, two (or three) water molecules, and a nitrate anion either as chelating agent or noncoordinated group.

Two parallel heterobimetallic chains are joined through the bpym ligand, which bridges pairs of trivalent rare-earth cations from neighboring rods, the separation across the bpym bridge being 6.9127(14) Å [Gd(1)···Gd(1)$^{(a)}$], 6.9409(8) Å [Tb(1)···Tb(1)$^{(a)}$], and 7.0037(7) Å [Sm1···Sm(1)$^{(a)}$; symmetry code (a) = $1-x$, $1-y$, $-z$], values which are slightly longer than those reported through the cyanide- and bpym-bridged $\{Fe_2^{III}Ln^{III}\}_2$ hexanuclear complexes.[14b]

A general supramolecular feature for compounds **1** and **2** is the aggregation of noncovalent layers in the *ab* plane through weak $\pi-\pi$ stacking interactions which are established between the aromatic rings of the outer [Fe(2)(phen)$CN)_4$] units of the ladders (Supporting Information, Figure S3). The values of the centroid−centroid distances are 4.0002(4) and 4.0691(4) Å (**1**) and 4.0376(5) and 4.0928(5) Å (**2**) whereas those of the angles between the normal to each aromatic ring and the centroid−centroid vector are 32.138(2)° and 35.565(22)° (**1**) and 31.2879(26)° and 35.368(26)° (**2**). The packing diagrams for **1**−**3** reveal the formation of N···O and O···O type hydrogen bonds with different topologies, depending on the lanthanide environment. The supramolecular layered structure in **1** is supplementarily supported by hydrogen bonds involving nitrate groups and crystallization water molecules (see Table 4 and in Supporting Information, Figure S4). Additional intraladder "rungs" are built by O(1W)···N(2)$^{(d)}$ hydrogen bonds [2.780(13) Å; (d) = $-x$, $1-y$, $-z$]. One coordinated water molecule is also involved in the intrachain hydrogen bonds toward a nitrate group from an adjacent $\{Ln(H_2O)_2(NO_3)$-$(bpym)(NC)_3\}$ moiety and also as hydrogen donor to one terminal cyanide ligand of the $\{Fe(2)(phen)(CN)_4\}$ entity [O(2W)···O(3A)$^{(c)}$ = 2.755(13) Å and O(2W)···N(7)$^{(c)}$ = 2.764(17) Å; (c) = $-1+x$, y, z] (Supporting Information, Figure S4). The changes from the coordination sphere of the terbium(III) cation in **2** determine the modification of the dimensionality in the network of hydrogen bonds (Supporting Information, Figure S5). The ladder structure is additionally supported by N···O type intrachain noncovalent interactions [O(1W)···N(2)$^{(d)}$ = 2.757(15) Å and O(2W)···N(7)$^{(c)}$ = 2.753(18) Å], the pathway of hydrogen bonds being restrained to a 1D arrangement. An inspection of the crystal packing of **3** shows a similar 1D noncovalent arrangement as in **2**, with an additional intrachain hydrogen bond running parallel to the crystallographic *a* axis, namely O(2w)···O(3A)$^{(c)}$.

[{Fe^{III}(phen)$(CN)_4$}$_2$$Pr_2^{III}$(bpym)$(NO_3)_4(H_2O)_2$]$_n$ (**4**). Compound **4** crystallizes in the monoclinic $P2_1/n$ space group. The structure is made up by repeating neutral heterobinuclear $[\{Fe^{III}(phen)(CN)(\mu\text{-}CN)Pr^{III}(bpym)_{1/2}(NO_3)_2(H_2O)\}(\mu\text{-}CN)_2]$ units which are connected to each other through two *trans*-cyanide groups along the crystallographic *c* axis. The resulting corrugated double-chains are further linked by the bis-chelated bpym molecules and generate layers, parallel to the *ac* plane (Figure 3). The corrugated chains describe some type of small "channels" across the *ab* plane, which are assembled from cyano-bridged $\{Fe_2^{III}Pr_2^{III}\}$-based heterobimetallic rings. Two distinct and alternating channel types are distinguished: those who are empty and the bpym-hosting ones. They are fused and give rise to the double-layered aspect of the structure (Figure 2c).

Each iron(III) cation is six-coordinate, with four cyanide ligands and one bidentate phen ligand building a somewhat distorted octahedral geometry as in **1**−**3**. The value of the angle subtended at the iron atom by the chelating phen ligand is 82.135(18)°. The distances associated to low-spin iron(III) paramagnetic center in **4** vary within the normal limits, 1.917(5)−1.951(5) and 1.988(4)−2.003(4) Å for Fe−C and Fe−N_{phen} bond lengths, respectively, values which agree with those reported for $\{Fe(phen)(CN)_4\}$ moiety in **1**−**3** and in the mononuclear species.[16g,h] The Fe−C−N bond angles are close to the strict linearity [175.8(4)−178.0(5)° (terminal cyanide groups) and 176.6(5)° (cyanide bridge)]. The $[Fe(1)(phen)$-$(CN)_4]^-$ anion adopts a tris-monodentate coordination mode toward the adjacent Pr(III) cations through three of its four cyanide groups. The Fe(1)−C(1)−N(1) unit assembles the asymmetric $[\{Fe^{III}(phen)(CN)_3(\mu\text{-}CN)Pr^{III}(bpym)$-$(NO_3)_2(H_2O)\}]$ heterobimetallic fragment, which is further intralinked by *trans*-C(3)−N(3) cyanide group to the neighboring binuclear units, building the $\{Fe_2^{III}Pr_2^{III}\}$-based rhombuses. The associated metal−metal distances are Fe(1)···Pr(1) = 5.6305(8) Å and Fe(1)···Pr(1)$^{(b)}$ = 5.3484(9) Å [symmetry code: (b) = $1-x$, $-y$, $1-z$)].

The second *trans*-cyanide link, Fe(1)−C(4)−N(4), connects successively the rhombuses along the crystallographic *c* axis, resulting in double-rods. The intrachain Fe(1)···Pr(1)$^{(c)}$ separation is 5.4976(9) Å [(c) = $1-x$, $-y$, $2-z$].

The bpym molecule acts as a bis-bidentate ligand toward the praseodymium(III) cations connecting the cyanide-based double chains into an extended array which grows in the *ac* plane. The separation between the rare-earth cations across the bridging bpym is 7.1013(8) Å [Pr(1)···Pr(1)$^{(a)}$; (a) = $2-x$, $-y$, $2-z$].

The praseodymium(III) ion is 10-coordinate with two bidentate nitrate groups, a water molecule, two nitrogen atoms from a bis-chelating bpym, and three cyanide-nitrogens building a distorted bicapped square antiprism geometry (mean bite value $b < 1$).[40] The largest metal to ligand distances are the Ln−N_{bpym} bonds [2.720(4) and 2.730(4) Å]. The Pr(III)−$O_{nitrate}$ bonds cover the range 2.578(4)−2.598(4) Å, being somewhat longer than the Pr(III)−O_{water} bond distance [2.495(3) Å]. As far as the cyanide-bridge pathways are concerned, the Pr(III)−N bond distances vary in the range 2.575(4) and 2.616(4) Å with significant departure from the linearity within the Pr−C−$N_{cyanide}$ fragments [Pr(1)−N(1)−C(1) = 167.1(4)°, Pr(1)−N(4)−C(4) = 153.0(4)°, and Pr(1)−N(3)−C(3) = 143.0(4)°]. The bent angles of the two

dx.doi.org/10.1021/ic302278q | *Inorg. Chem.* 2013, 52, 1525−1537

trans cyanide bridges, in combination with the nearly linear Fe(1)−C(3)−N(3) [177.4(4)°] and Fe(1)−C(4)−N(4) [178.0(5)°] set of atoms, determine the wave-like shape of the double-chains, and further lead to the bilayered aspect of the 2D structure (Figure 3c). As in **1**−**3**, an inversion center is located in the middle point of the inter-ring carbon−carbon bond of the bpym molecule.

Compounds **1**−**4** contain cyanide- and bpym-bridged $\{Fe_2^{III}Ln^{III}\}_2$ moieties whose topology and structural parameters are similar to those in the hexanuclear series of compounds, $[\{Fe^{III}(phen)(CN)_3(\mu\text{-}CN)\}_4Ln_2^{III}(NO_3)_2(H_2O)_6(\mu\text{-}bpym)]\cdot nH_2O$ [Ln = Eu, Gd, Dy, and Ho; n = 8 (Eu, Dy, and Ho) and n = 11 (Gd)].[14b] Focusing on the role played by the bpym ligands on the structural topology in compounds **1**−**4**, one can easily note that the bis-chelating polyazine ligand acts differently in **1**−**3** compared to **4**. So, bpym has only a tailoring role in **1**−**3** joining two cyanide-based chains into ladders, the 1D structure being preserved. In the case of **4**, the bis-bidentate bpym acted, together with cyanide ligands, as expanding connectors, linking the neighboring corrugated ladders into extended layers. The formation of arrays in **4** is most likely favored by the higher coordination number (10) of the praseodymium(III) ion compared to the heavier lanthanide series [Sm(III), Gd(III), and Tb(III)] (Figure 4). The interference of the ionic radii cannot be excluded, with the trivalent praseodymium cation having the largest value.

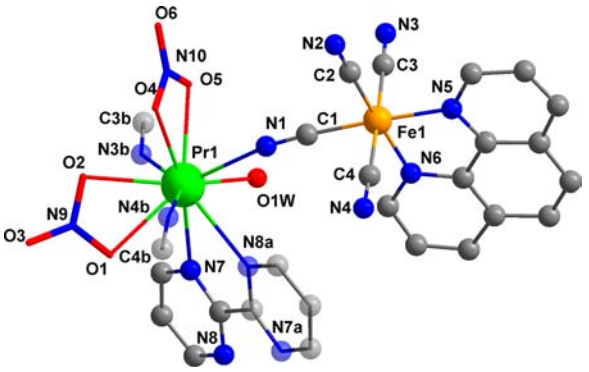

Figure 4. View of a fragment of **4**, showing the most important atom numbering. The asymmetric unit is represented as spheres, except the nitrate group that is represented as sticks. The atoms generated by symmetry operations have been drawn in the transparent mode.

Magnetic Properties of the Compounds 1−4. Because of the difficulties in the analysis and interpretation of the magnetic properties of the mixed low spin Fe^{3+}−Ln^{3+} pairs, let us make some considerations prior to the presentation, analysis, and discussion of the magnetic data of **1**−**4**.

The different factors that challenge the analysis of the magnetic properties of mixed low spin Fe^{3+}−Ln^{3+} systems are the following: (i) the first-order angular momentum of the low-spin iron(III) and the trivalent lanthanide ion (with the exception of the Gd^{3+} and the diamagnetic La^{3+} and Lu^{3+} cations) which prevents the use of the spin-only formalism; (ii) the value of the crystal field splitting of the rare-earth element which is usually on the order of kT at room temperature so that the thermal population of the Stark levels has to be implicitly taken into account; (iii) and the inner nature of the 4f orbitals with respect to the 3d ones which is responsible for the weak magnetic exchange interactions observed in 3d−4f systems and whose nature and magnitude can be masked by the orbital contributions, crystal field effects, and intermolecular interactions. This is why in order to extract quantitative information in such systems, a more empirical method has been often used in the cyanide-bridged 3d−4f complexes where one orbital contribution is simply removed by comparing the magnetic data of the isostructural $M(3d)_{paramagnetic}$−$M(4f)_{diamagnetic}$, $M(3d)_{paramagnetic}$−$M(4f)_{paramagnetic}$ and $M(3d)_{diamagnetic}$−$M(4f)_{paramagnetic}$ compounds (in particular, the low spin Fe^{3+} and the paramagnetic Ln^{3+} are replaced by Co^{3+} and diamagnetic Ln^{3+}, respectively).[2e,f,6a,b,7b−d,f,g,10d] Unfortunately, the strategy of substituting the paramagnetic lanthanide centers of **1**−**4** by the diamagnetic La^{3+} did not provide single crystals. The above-mentioned difficulties are increased in the magnetic study of the ladder-like (**1**−**3**) and sheet-like (**4**) compounds of the present work because of the occurrence of two posible exchange pathways, the single cyanide bridge between the low spin Fe^{3+} and the Ln^{3+} and the bis-bidentate bpym between the Ln^{3+} centers [Ln = Gd (**1**), Tb (**2**), Sm (**3**), and Pr (**4**)].

As far as the magnetic coupling with rare-earth elements through bridging bpym is concerned, the magneto-structural data are practically limited to two centrosymmetic compounds of formula $[\{GdL_3\}_2(\mu\text{-bpym})]$ (HL = dimethyl-*N*-trichloroacetylamidophosphate)[28d] and $[\{Fe^{III}(phen)(CN)_3(\mu\text{-}CN)\}_4Gd_2(NO_3)_2(H_2O)_6(\mu\text{-bpym})]\cdot 11H_2O$.[14b]

The former one is a binuclear complex where the two Gd(III) ions are connected through bis-bidentate bpym whereas the second one is a hexanuclear compound whose structure consists of two cyanide-bridged $\{Fe^{III}{}_2Gd^{III}\}$ heterobimetallic moieties which are linked by a bis-bidentate bpym between the two gadolinium(III) cations. The magnetic interaction through the bpym bridge in both cases is J = −0.039 cm^{-1} (the Hamiltonian defined as $\mathbf{H} = -J\mathbf{S}_{Gd1}\cdot\mathbf{S}_{Gd2}$). The magneto-structural studies on single cyanide-bridged low spin Fe^{3+}−Ln^{3+} systems are really abundant, and here we limit ourselves to the results with Ln = Pr, Sm, Gd, and Tb which are summarized in Table 5. An inspection of Table 5 shows either negligible or weak ferro-/antiferromagnetic interactions between the low spin Fe^{3+} and the paramagnetic Ln^{3+} through the single cyanide bridge.

Magnetic Properties of 1. The temperature dependence of the $\chi_M T$ product of compound **1** (χ_M is the magnetic suceptibility per $Fe^{III}{}_2Gd^{III}$ unit) is shown in Figure 5.

$\chi_M T$ at 295 K is 9.15 $cm^3\ mol^{-1}$ K, a value which is as expected for two magnetically noninteracting low-spin iron(III) ions, with a significant orbital contribution (S_{Fe} = $^1/_2$ with spin−orbit coupling of the $^2T_{2g}$ ground term) plus one magnetically isolated Gd(III) ion with a $^8S_{7/2}$ low-lying state ($4f^7$, J = $^7/_2$, L = 0, and S = $^7/_2$) being located at some 10^4 cm^{-1} below the first excited state. Upon cooling, $\chi_M T$ decreases quasilinearly in the high temperature range. This decrease is due to the spin−orbit coupling effects of the low-spin iron(III) ions. Below 40 K, $\chi_M T$ exhibits an abrupt decrease to reach a value of 7.0 $cm^3\ mol^{-1}$ K at 1.9 K. Such a decrease cannot be due to zero-field splitting effects of the Gd(III) ion because of its practically isotropic character. Then, intra- or intermolecular antiferromagnetic interactions in **1** are responsible for this last decrease, the value of $\chi_M T$ at 1.9 K being well below that resulting from the sum of a magnetically isolated gadolinium(III) center (7.875 $cm^3\ mol^{-1}$ K with g_{Gd} = 2.0) and two magnetically noninteracting low spin iron(III) ions [values of $\chi_M T$ varying in the range 0.45−0.53 $cm^3\ mol^{-1}$ K at 1.9 K per mol of iron(III) in the family $[Fe^{III}(AA)(CN_4)]^-$ precursors (AA = α-diimine type ligand)].[2e,7b−d,14b,16g,15e] The magnet-

dx.doi.org/10.1021/ic302278q | *Inorg. Chem.* 2013, 52, 1525−1537

Table 5. Selected Magneto-Structural Data for Single Cyanide-Bridged Fe^{III}–Ln^{III} Complexes (Ln = Pr, Sm, Gd, and Tb)

structural type	Fe–(μ-CN)–Ln distances (Å)	magnetic behavior	ref
	Pr–Fe		
binuclear	5.580	negligible interactions	10d
trinuclear	5.608	negligible interactions	7c
binuclear	5.691	weak F	2f
2D	5.634	weak AF	2f
	Sm–Fe		
binuclear		negligible interactions	10d
binuclear	5.373(1)-5.601(1)	negligible interactions	2c
1D	5.446	negligible interactions	7g
1D	5.483	F	2e
1D	5.459	F	2e
1D	5.329	F	2e
1D	5.612	ferrimagnet	7b
2D	5.47–5.58	ferrimagnet	2b
2D	5.363(2)-5.555(2)	negligible interactions	2c
binuclear	5.645	weak F	2f
	Gd–Fe		
binuclear		AF	8b
hexanuclear	5.5223(7)–5.4509(7)	AF	14b
1D	5.564	weak AF	7b
1D	5.593(1)	weak F	2k
1D	5.563	weak AF	7f
2D		weak AF	2b
	Tb–Fe		
binuclear		F	10d
1D	5.464, 5.565	weak AF	7d
1D	5.513	negligible interaction	2e
1D	5.574(2)	negligible interaction	2k
2D	5.47–5.53	negligible interaction	2b

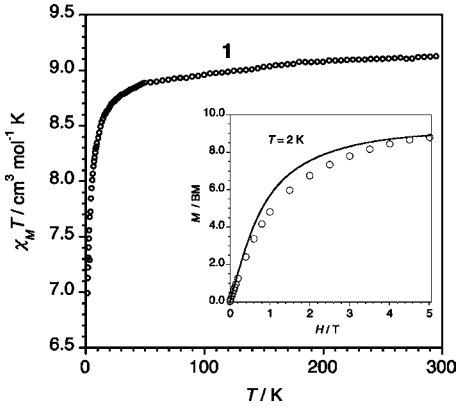

Figure 5. $\chi_M T$ vs T plot for **1**. The inset shows the magnetization against H plot for **1** at 2.0 K: (○) experimental; (—) Brillouin function for a magnetically noninteracting set of one gadolinium(III) ($S_{Gd} = {}^7/_2$ with $g = 2.0$) and two low-spin iron(III) ($S_{Fe} = {}^1/_2$ with $g = 2.1$) ions.

ization (M) versus H plot at 2.0 K for **1** (see inset of Figure 5) also supports the occurrence of an overall antiferromagnetic interaction in **1**, the values of the magnetization being always below those of the Brillouin function for a set of magnetically isolated one gadolinium(III) and two low-spin iron(III) ions.

Although there is no model to analyze the magnetic properties of a ladder-like spin topology like that of **1** with two magnetic couplings, one through the rungs [bridging bpym between the Gd(III) ions] and the other across the rails [single cyanide-bridge between Fe(III) and Gd(III)], the hexanuclear compound $[\{Fe^{III}(phen)(CN)_3(\mu\text{-}CN)\}_4Gd_2(NO_3)_2(H_2O)_6(\mu\text{-}bpym)]\cdot 11H_2O$[14b] which reproduces a fragment of this ladder-like chain with quasi-identical intramolecular metal–metal separations [6.7971(6) Å (hexanuclear) and 6.9127(14) Å (**1**) for Gd–(μ-bpym)–Gd and 5.5223(7)/5.4509(7) Å (hexanuclear) and 5.3882(16)/5.3871(16) Å (**1**) for Fe–(μ-CN)–Gd] can be taken as an orientative model for the magnetic couplings in **1**. At this respect, the magnetic interactions for the Fe^{III}–(μ-CN)–Gd^{III} ($J = -0.49$ cm^{-1}) and Gd^{III}(μ-bpym)Gd^{III} ($J = -0.039$ cm^{-1}) fragments which were found in the hexanuclear compound can be reasonably expected for **1**.

Magnetic Properties of **2**. The temperature dependence of the $\chi_M T$ product of compound **2** (χ_M is the magnetic suceptibility per $Fe^{III}{}_2Tb^{III}$ unit) is shown in Figure 6.

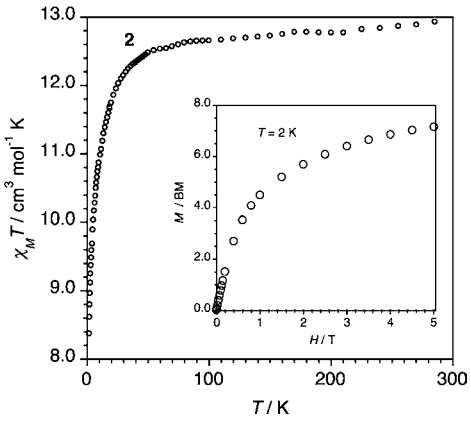

Figure 6. $\chi_M T$ vs T plot for **2**. The inset shows the magnetization against H plot for **2** at 2.0 K.

$\chi_M T$ at 290 K is 12.94 cm^3 mol^{-1} K, a value which is as expected for two magnetically noninteracting low-spin iron(III) ions with a significant orbital contribution plus one magnetically isolated Tb(III) ion with a $^7F_6$ low-lying state ($4f^8$, $J = 6$, $L = 3$, $g_J = {}^3/_2$, and $S = 3$), $\chi_M T$ being 11.81 cm^3 mol^{-1} K [per one terbium(III) ion]. Upon cooling, $\chi_M T$ decreases practically linearly until 70 K, and it further decreases sharply to 8.35 cm^3 mol^{-1} K at 1.9 K. The magnetization versus H plot for **2** at 2.0 K (see inset of Figure 6) is far from reaching the saturation, and the magnetization attains a value of 7.3 μ_B at 5 T (the maximum available magnetic field in our device). The decrease of $\chi_M T$ in **2** is governed by the spin–orbit coupling effects of the low-spin iron(III) ions plus the thermal depopulation of the Stark levels of the terbium(III) ion, with these features making it impossible to estimate the $\chi_M T$ value of the Tb(III) at 2.0 K. This circumstance together with the lack of data in the literature concerning the magnetic interactions through the two intrachain exchange pathways occurring in **2** [low spin Fe^{3+}–(μ-CN)–Tb^{3+} and Tb^{3+}–(μ-bpym)–Tb^{3+}] does not allow us to go beyond in our analysis about the nature and magnitude of the magnetic coupling (if any) for this compound. By the way, one can see in Table 5 that negligible magnetic interactions were quoted for the low spin Fe^{3+}–(μ-CN)–Tb^{3+} fragment in most of the explored examples.

Magnetic Properties of **3**. The temperature dependence of the $\chi_M T$ product of compound **3** (χ_M is the magnetic suceptibility per $Fe^{III}{}_2Sm^{III}$ unit) is shown in Figure 7. $\chi_M T$ at

dx.doi.org/10.1021/ic302278q | Inorg. Chem. 2013, 52, 1525–1537

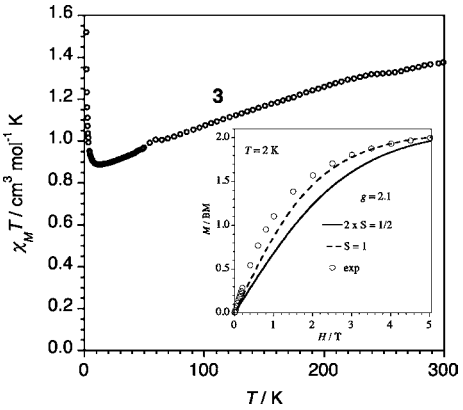

Figure 7. $\chi_M T$ vs T plot for **3**. The inset shows the magnetization against H plot for **3** at 2.0 K: (○) experimental; (—) Brillouin function for two magnetically noninteracting spin doublets with g = 2.1; (---) Brillouin function for a spin triplet with g = 2.1.

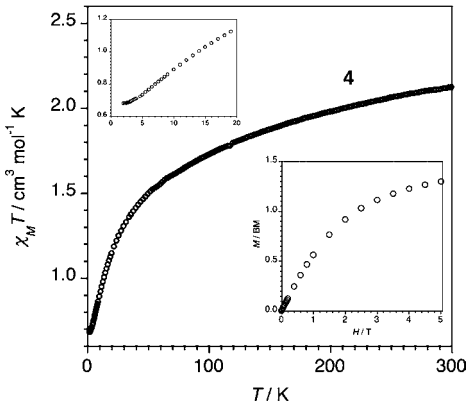

Figure 8. $\chi_M T$ vs T plot for **4** (inset: M vs H plot). The upper inset shows the low temperature region of the $\chi_M T$ against T plot. The lower inset is the M vs H plot for **4** at 2.0 K.

300 K is 1.38 $cm^3\ mol^{-1}$ K, a value which is as expected for two magnetically noninteracting low-spin iron(III) ions with a significant orbital contribution [values in the range 0.54−0.68 $cm^3\ mol^{-1}$ K per one low-spin iron(III)] plus one magnetically isolated Sm(III) ion with a $^6H_{5/2}$ low-lying state ($4f^5$, $J = {}^5/_2$, L = 5, $g_J = {}^2/_7$, and $S = {}^5/_2$), with $\chi_M T$ being ca. 0.09 $cm^3\ mol^{-1}$ K [per one Sm(III) ion]. Upon cooling, $\chi_M T$ decreases to reach a minimum value of 0.88 $cm^3\ mol^{-1}$ K at 10 K, and then it sharply increases to 1.52 $cm^3\ mol^{-1}$ K at 1.9 K.

The decrease of $\chi_M T$ in the high temperature domain for **3** is mainly due to the orbital contribution of the two low-spin iron(III) ions whereas the increase of $\chi_M T$ below 10 K clearly supports a weak overall ferromagnetic coupling. The occurrence of this ferromagnetic interaction can be observed in the M against H plot for **3** at 2.0 K (see inset of Figure 7) where the experimental data are always above the Brillouin function for two magnetically isolated spin doublets ($S_{Fe} = {}^1/_2$ with g_{Fe} = 2.1) and even somewhat above the Brillouin function for a S = 1 with g = 2.1.

Because of the extremely weak spin density on the Sm^{3+} ion at low temperatures, the observed increase of $\chi_M T$ in Figure 7 could be due either to (i) a ferrromagnetic interaction beween the spin doublets of the low-spin iron(III) ions and the small spin density of the samarium(III) cation along the rods (by neglecting the magnetic interaction through the bis-bidentate bpym) or (ii) an antiferromagnetic interaction between the low-spin iron(III) ions and the small spin density of the samarium(III) cation that would result in a ferrimagnetic chain. In both cases, the total spin per $Fe^{III}_2Sm^{III}$ unit would be S_T = 1 ($S_T = 2 \times S_{Fe} \pm S_{Sm} \approx 1$). We cannot make a choice between these two possibilities at the present stage of the knowledge, but the parallel alignment of the local spin doublets in **3** is ensured.

Magnetic Properties of **4**. The temperature dependence of the $\chi_M T$ product of compound **4** (χ_M is the magnetic suceptibility per $Fe^{III}Pr^{III}$ unit) is shown in Figure 8.

$\chi_M T$ at 300 K is 2.15 $cm^3\ mol^{-1}$ K, a value which agrees with that expected for one magnetically noninteracting low-spin iron(III) ion with a significant orbital contribution [values in the range 0.54−0.68 $cm^3\ mol^{-1}$ K per one low-spin iron(III)] plus one magnetically isolated Pr(III) ion with a $^3H_4$ low-lying state ($4f^2$, J = 4, L = 5, $g_J = {}^4/_5$, and S = 1), $\chi_M T$ being 1.60 $cm^3\ mol^{-1}$ K [per one praseodymium(III) ion]. Upon cooling, $\chi_M T$ continuously decreases to reach an incipient plateau with $\chi_M T$ = 0.65 $cm^3\ mol^{-1}$ K at 1.9 K (see upper inset of Figure 8). The decrease of $\chi_M T$ in **4** is mainly due to spin−orbit coupling of the low-spin iron(III) center plus the ligand field effects of the praseodymium(III) cation. As far as the incipient plateau in the low temperature region is concerned, its presence is indicative that the magnetic moment of the Pr(III) vanishes at low temperatures, and so, the value of $\chi_M T$ is basically determined by a quasimagnetically isolated low-spin iron(III) center. This conclusion receives additional support by the field dependence of the magnetization for **4** at 2.0 K (see lower inset of Figure 8): the magnetization tends to a quasisaturation value of 1.3 μ_B at 5 T in agreement with the occurrence of a $S = {}^1/_2$ with g = 2.1 plus a small contribution to the magnetization of the Pr(III) cation. These results unambiguously support the lack of a significant magnetic coupling through the single cyanide- and bis-bidentate bpym bridges in the (low spin) Fe^{3+}−(μ-CN)−Pr^{3+} and Pr^{3+}−(μ-bpym)−Pr^{3+} of **4**.

CONCLUSIONS

The examples here enrich the very limited family of d−f hybrid PB analogues and show that a combined strategy involving auxiliary ligands (bpym) and heteroleptic metallocyanate precursors lead, in reaction with f cations, to extended cyanide- and bpym-bridged heterobimetallic Fe^{III}−Ln^{III} assemblies with interesting structural topologies. The anhydrous reaction conditions were crucial in the development of double-chains with ladder-like topology and a layered structure. The formation of the sheet-like structure is most likely related with the higher coordination number (10) and the greater ionic radius of the Pr(III) cation. The possible influence of the lanthanide contraction is observed also for compounds **1**−**3** in which the slight differences in the surrounding of the lanthanide(III) cations influenced the topology of the hydrogen bonded network and the dimensionality. The auxiliary bis-bidentate poliazine ligand in **1**−**4** provided an exchange pathway between two adjacent lanthanide(III) cations which coexists with that through the cyanide bridges.

The analysis of the magnetic data of **1** reveals the occurrence of a weak antiferromagnetic coupling for Fe^{III}−CN−Ln^{III} pair and very weak antiferromagnetic interaction between the two gadolinium(III) cations across the bpym bridge. An overall weak ferromagnetic interaction is observed for the Sm(III) derivative (**3**) whereas very weak or no magnetic interactions for **2** and **4** complete the picture of magnetic properties for the present new series of Fe^{III}−Ln^{III} systems. Alternative mixed d−f

dx.doi.org/10.1021/ic302278q | Inorg. Chem. 2013, 52, 1525−1537

species with a similar structural topology but exhibiting "accessible" magnetic behavior [for example cyanide- and bpym-bridged Co^{3+}-Ln^{3+} systems and Ln^{3+}-(μ-bpym)Ln^{3+}] are envisaged in order to elucidate and model the complexity of the magnetic exchange interaction, via cyanide and bpym bridges, between the low spin Fe^{3+} and Ln^{3+} pairs of cations. The foregoing results brought us more closely to better control of the unexpected chemistry of the 4f cations and also to open new perspectives in designing low-dimensional d−f hybrid PB analogues.

■ ASSOCIATED CONTENT

Supporting Information

Structural drawings of **1**−**3** (Figure S1), the coordination polyhedra of the lanthanide(III) ions from **1** and **2** (Figure S2), fragments of the packing diagrams for **1** and **2**, showing the $\pi-\pi$ stacking interactions (Figure S3) and the hydrogen bonds (Figures S4 and S5); X-ray crystallographic files (CIF) for compounds **1**−**4**. This material is available free of charge via the Internet at http://pubs.acs.org. Crystallographic files also available upon application to the Cambridge Crystallographic data Centre, 12 Union Road, Cambridge CB2 1EZ, U.K. [fax (+44)1223−336−033; e-mail deposit@ccdc.cam.ac.uk]: CCDC 903519 (**1**), 903520 (**2**), 903521 (**3**), and 903522 (**4**).

■ AUTHOR INFORMATION

Corresponding Author

*E-mail: diana.visinescu@gmail.com (D.V.); miguel.julve@uv.es (M.J.).

Notes

The authors declare no competing financial interest.

■ ACKNOWLEDGMENTS

Financial support from the Romanian National Authority for Scientific Research, CNCS-UEFISCDI, Project PN-II-RU-TE-2011-3-0126, the Spanish MICINN (Projects CTQ2010-15364, MAT2010-16981, MAT2011-2733-C02-02, CSD2007-00010, and "Factoría de Crystalización" Consolider-Ingenio2010, CSD2006-00015), and the Generalitat Valenciana (PROMETEO2009/108 and ISIC/2012/002) is gratefully acknowledged.

■ REFERENCES

(1) (a) Shore, S. G.; Knoeppel, D. W.; Deng, H.; Liu, J.; White, J. P., III; Chun, S.-H. *J. Alloys Compd.* **1997**, *249*, 25. (b) Sakamoto, M.; Manseki, K.; Okawa, H. *Coord. Chem. Rev.* **2001**, *219*−*221*, 379. (c) Plečnik, C. E.; Liu, S.; Shore, S. G. *Acc. Chem. Res.* **2003**, *36*, 499. (d) Gu, X.; Xue, D.; Ratajczak, H. *J. Mol. Struct.* **2008**, *887*, 56. (e) Benelli, C.; Gatteschi, D. *Chem. Rev.* **2002**, *102*, 2369. (f) Andruh, M.; Costes, J.-P.; Diaz, C.; Gao, S. *Inorg. Chem.* **2009**, *48*, 3342. (g) Ward, M. D. *Coord. Chem. Rev.* **2007**, *251*, 1663. (h) Chen, F.-F.; Chen, Z.-Q.; Bian, Z.-Q.; Huang, C.-H. *Coord. Chem. Rev.* **2010**, *254*, 991.

(2) (a) Tanase, S.; Reedijk, J. *Coord. Chem. Rev.* **2006**, *250*, 2501 and references therein. (b) Zhang, Y.-Z.; Duan, G.-P.; Sato, O.; Gao, S. *J. Mater. Chem.* **2006**, *16*, 2625. (c) Chen, W.-T.; Wang, M.-S.; Cai, L.-Z.; Xu, G.; Akitsu, T.; Akita-Tanaka, M.; Guo, G.-C.; Huang, J.-S. *Cryst. Growth Des.* **2006**, *6*, 1738. (d) Akitsu, T.; Einaga, Y. *Polyhedron* **2006**, *25*, 2655. (e) Lopez, N.; Prosvirin, A.; Chifotides, H. T.; Dunbar, K. R. *Dalton Trans.* **2007**, 878. (f) Chen, W.-T.; Guo, G.-C.; Wang, M.-S.; Xu, G.; Cai, L.-Z.; Akitsu, T.; Akita-Tanaka, M.; Matsushita, A.; Huang, J.-S. *Inorg. Chem.* **2007**, *46*, 2105. (g) Figuerola, A.; Tangoulis, V.; Sanakis, Y. *Chem. Phys.* **2007**, *334*, 204. (h) Sun, X.-R.; Chen, Z.-D.; Wang, M.-W.; Wang, B.-W.; Yan, F.; Cheung, K.-K. *Chin. J. Chem.* **2007**, *25*, 329. (i) Li, J. R.; Chen, W.-T.; Tong, M. L.; Guo, C. G.; Tao, Y.; Yu, Q.; Song, W.-C.; Bu, X.-H. *Cryst. Growth Des.* **2008**, *8*, 2780. (j) Zhu, X.; Wong, W.-K.; Guo, J.; Wong, W.-Y.; Zhang, J.-P. *Eur. J. Inorg. Chem.* **2008**, 3515. (k) Wilson, D. C.; Liu, S.; Chen, X.; Meyers, E. A.; Bao, X.; Prosvirin, A. V.; Dunbar, K. R.; Hadad, C. M.; Shore, S. G. *Inorg. Chem.* **2009**, *48*, 5725. (l) Svendsen, H.; Overgaard, J.; Chevallier, M.; Collet, E.; Iversen, B. B. *Angew. Chem., Int. Ed.* **2009**, *48*, 2780. (m) Chen, W.-T.; Wu, A.-Q.; Guo, G.-C.; Wang, M.-S.; Cai, L.-Z.; Huang, J.-S. *Eur. J. Inorg. Chem.* **2010**, 2826. (n) Gurunatha, K. L.; Mostafa, G.; Ghoshal, D.; Maji, T. K. *Cryst. Growth Des.* **2010**, *10*, 2483. (o) Svendsen, H.; Overgaard, J.; Chevalier, M.; Collet, E.; Chen, Y.-S.; Jensen, F.; Iversen, B. B. *Chem.—Eur. J.* **2010**, *16*, 7215. (p) Svendsen, H.; Vogel Jørgensen, M. R.; Overgaard, J.; Chen, Y.-S.; Chastanet, G.; Létard, J.-F.; Kato, K.; Takata, M.; Iversen, B. B. *Inorg. Chem.* **2011**, *50*, 10974.

(3) (a) Ohba, M.; Ōkawa, H. *Coord. Chem. Rev.* **2000**, *198*, 313. (b) Černák, J.; Orendáč, M.; Potočňák, I.; Chomič, J.; Orendáčová, A.; Skoršepa, J.; Feher, A. *Coord. Chem. Rev.* **2002**, *224*, 51. (c) Shatruk, M.; Avendano, C.; Dunbar, K. *Prog. Inorg. Chem.* **2009**, *56*, 155.

(4) (a) Rinehart, J. D.; Long, J. R. *Chem. Sci.* **2011**, *2*, 2078. (b) Sorace, L.; Benelli, C.; Gatteschi, D. *Chem. Soc. Rev.* **2011**, *40*, 3092.

(5) (a) Grant, A. J.; James, C. *J. Am. Chem. Soc.* **1917**, *39*, 933. (b) Prandtl, W.; Mohr, S. *Z. Anorg. Allg. Chem.* **1938**, *236*, 243. (c) Bailey, W. E.; Williams, R. J.; Milligan, W. O. *Acta Crystallogr.* **1973**, *B29*, 1365. (d) Kietaibl, H.; Petter, W. *Helv. Phys. Acta* **1974**, *47*, 425. (e) Hulliger, H.; Landolt, M.; Vetsch, H. *J. Solid State Chem.* **1976**, *18*, 307. (f) Hulliger, H.; Landolt, M.; Vetsch, H. *J. Solid State Chem.* **1976**, *18*, 283. (g) Petter, W.; Gramlich, V.; Hulliger, F. *J. Solid State Chem.* **1989**, *82*, 161. (h) Zhou, X.; Wong, W.-T.; Faucher, M. D.; Tanner, P. A. *J. Solid State Chem.* **2008**, *181*, 3057.

(6) (a) Yan, B.; Wang, H.-D.; Chen, Z.-D. *Polyhedron* **2001**, *20*, 591. (b) Yan, B.; Chen, Z. *Helv. Chim. Acta* **2001**, *84*, 817. (c) Sun, X.-R.; Chen, Z.-D.; Yan, F.; Gao, S.; Cheung, K.-K.; Che, C.-M.; Zhang, X.-X. *J. Cluster Sci.* **2002**, *13*, 103. (d) Kou, H. -Z.; Gao, S.; Wang, R.-J. *Acta Crystallogr.* **2002**, *C58*, m325. (e) Kou, H. -Z.; Gao, S.; Li, C.-H.; Liao, D.-Z.; Zhou, B.-C.; Wang, R.-J.; Li, Y. *Inorg. Chem.* **2002**, *41*, 4756. (f) Yan, B.; Song, Y. *J. Coord. Chem.* **2004**, *57*, 49.

(7) (a) Figuerola, A.; Díaz, C.; El Fallah, M. S.; Ribas, J.; Maestro, M.; Mahía, J. *Chem. Commun.* **2001**, 1204. (b) Figuerola, A.; Díaz, C.; Ribas, J.; Tangoulis, V.; Sangregorio, C.; Gatteschi, D.; Maestro, M.; Mahía, J. *Inorg. Chem.* **2003**, *42*, 5274. (c) Figuerola, A.; Ribas, J.; Llunell, M.; Casanova, D.; Maestro, M.; Alvarez, S.; Díaz, C. *Inorg. Chem.* **2005**, *44*, 6939. (d) Figuerola, A.; Ribas, J.; Casanova, D.; Maestro, M.; Alvarez, S.; Díaz, C. *Inorg. Chem.* **2005**, *44*, 6949. (e) Yi, T.; Gao, S.; Chen, X.-W.; Yan, C.-H.; Li, B. G. *Acta Crystallogr.* **1998**, *C54*, 41. (f) Koner, R.; Drew, M. G. B.; Figuerola, A.; Díaz, C.; Mohanta, S. *Inorg. Chim. Acta* **2005**, *358*, 304. (g) Figuerola, A.; Ribas, J.; Solans, X.; Font-Bardía, M.; Maestro, M.; Díaz, C. *Eur. J. Inorg. Chem.* **2006**, *9*, 1846.

(8) (a) Tanase, S.; Andruh, M.; Müller, A.; Schmidtmann, M.; Mathonière, C.; Rombaut, G. *Chem. Commun.* **2001**, 1084. (b) Stoian, S.; Paraschiv, C.; Kiritsakas, N.; Lloret, F.; Münck, E.; Bominaar, E. L.; Andruh, M. *Inorg. Chem.* **2010**, *49*, 3387.

(9) Ma, B. Q.; Gao, S.; Su, G.; Xun, G. X. *Angew. Chem., Int. Ed.* **2001**, *40*, 434.

(10) (a) Kou, H.-Z.; Yang, G.-M.; Liao, D.-Z.; Cheng, P.; Jiang, Z.-H.; Yan, S.-P.; Huang, X.-Y.; Wang, G.-L. *J. Chem. Crystallogr.* **1998**, *28*, 303. (b) Kautz, J. A.; Mullica, D. F.; Cunningham, B. P.; Combs, R. A.; Farmer, J. M. *J. Mol. Struct.* **2000**, *523*, 175. (c) Mullica, D. F.; Farmer, J. M.; Cunningham, B. P.; Kautz, J. A. *J. Coord. Chem.* **2000**, *9*, 239. (d) Figuerola, A.; Díaz, C.; Ribas, J.; Tangoulis, V.; Granell, J.; Lloret, F.; Mahía, J.; Maestro, M. *Inorg. Chem.* **2003**, *42*, 641. (e) Li, G.; Akitsu, T.; Sato, O.; Einaga, Y. *J. Am. Chem. Soc.* **2003**, *125*, 12396. (f) Li, G.; Akitsu, T.; Sato, O.; Einaga, Y. *Hyperfine Interact.* **2004**, *156/157*, 143. (g) Li, G.; Akitsu, T.; Sato, O.; Einaga, Y. *J. Coord. Chem.* **2004**, *57*, 189. (h) Li, G.; Akitsu, T.; Sato, O.; Einaga, Y. *J. Coord. Chem.* **2004**, *57*, 855. (i) Dai, Y.; Chen, X.-Y.; Cheng, P.; Liao, D.-Z.; Yan, S. P.; Jiang, Z.-H. *Transition Met. Chem.* **2004**, *29*, 12. (j) Dong,

W.; Ouyang, Y.; Xu, J.-X.; Liao, D.-Z.; Yan, S.-P. *J. Coord. Chem.* **2008**, *61*, 997. (k) Li, G.; Yan, P.; Sato, O.; Einaga, Y. *J. Solid State Chem.* **2005**, *178*, 36.
(11) (a) Kou, H. Z.; Gao, S.; Sun, B. W.; Zhang, J. *Chem. Mater.* **2001**, *13*, 1431. (b) Kou, H. Z.; Gao, S.; Jin, X. L. *Inorg. Chem.* **2001**, *40*, 6295.
(12) (a) Yeung, W. F.; Lau, T. C.; Wang, X. Y.; Gao, S.; Szeto, L.; Wong, W. T. *Inorg. Chem.* **2006**, *45*, 6756. (b) Baca, S. G.; Adams, H.; Sykes, D.; Faukner, S.; Ward, M. D. *Dalton Trans.* **2007**, 2149. (c) Herrera, J.-M.; Pope, S. G. A.; Adams, H.; Faulkner, S.; Ward, M. D. *Inorg. Chem.* **2006**, *45*, 3895. (d) Baca, S. G.; Pope, S. G. A.; Adams, H.; Ward, M. D. *Inorg. Chem.* **2008**, *47*, 3736. (e) Davies, G. M.; Pope, S. G. A.; Adams, H.; Faukner, S.; Ward, M. D. *Inorg. Chem.* **2005**, *44*, 4656.
(13) (a) Alexandru, M.-G.; Visinescu, D.; Madalan, A. M.; Lloret, F.; Julve, M.; Andruh, M. *Inorg. Chem.* **2012**, *51*, 4906. (b) Palacios, M. A.; Mota, A. J.; Ruiz, J.; Hanninen, M. M.; Sillanpaa, R.; Colacio, E. *Inorg. Chem.* **2012**, *51*, 7010.
(14) (a) Visinescu, D.; Toma, L. M.; Fabelo, O.; Ruiz-Pérez, C.; Lloret, F.; Julve, M. *Polyhedron* **2009**, *28*, 851. (b) Visinescu, D.; Fabelo, O.; Ruiz-Pérez, C.; Lloret, F.; Julve, M. *CrystEngComm* **2010**, *12*, 2454.
(15) (a) Lescouëzec, R.; Toma, L. M.; Vaissermann, J.; Verdaguer, M.; Delgado, F. S.; Ruiz-Pérez, C.; Lloret, F.; Julve, M. *Coord. Chem. Rev.* **2005**, *249*, 2691. (b) Toma, L. M.; Lescouëzec, R.; Pasán, J.; Ruiz-Pérez, C.; Vaissermann, J.; Cano, J.; Carrasco, R.; Wernsdorfer, W. *J. Am. Chem. Soc.* **2006**, *128*, 4842. (c) Toma, L. M.; Ruiz-Pérez, C.; Lloret, F.; Julve, M. *Inorg. Chem.* **2012**, *51*, 1216. (d) Toma, L. M.; Ruiz-Pérez, C.; Pásan, J.; Wernsdorfer, W.; Lloret, F.; Julve, M. *J. Am. Chem. Soc.* **2012**, *134*, 15265. (e) Toma, L. M.; Pasán, J.; Ruiz-Pérez, C.; Lloret, F.; Julve, M. *Dalton Trans.* **2012**, *41*, 13716.
(16) (a) Lescouëzec, R.; Lloret, F.; Julve, M.; Vaissermann, J.; Verdaguer, M. *Inorg. Chem.* **2002**, *41*, 818. (b) Toma, L. M.; Lescouëzec, R.; Lloret, F.; Julve, M.; Vaissermann, J.; Verdaguer, M. *Chem. Commun.* **2003**, 1850. (c) Lescouëzec, R.; Vaissermann, J.; Ruiz-Pérez, C.; Lloret, F.; Carrasco, R.; Julve, M.; Verdaguer, M.; Dromzée, Y.; Gatteschi, D.; Wernsdorfer, W. *Angew. Chem., Int. Ed.* **2003**, *42*, 1483. (d) Toma, L. M.; Lescouëzec, R.; Toma, L. D.; Lloret, F.; Julve, M.; Vaissermann, J.; Andruh, M. *J. Chem. Soc., Dalton Trans.* **2002**, 3171. (e) Toma, L. M.; Lescouëzec, R.; Uriel, S.; Llusar, R.; Ruiz-Pérez, C.; Vaissermann, J.; Lloret, F.; Julve, M. *Dalton Trans.* **2007**, 3690. (f) Toma, L. M.; Delgado, F. S.; Ruiz-Pérez, C.; Carrasco, R.; Cano, J.; Lloret, F.; Julve, M. *Dalton Trans.* **2004**, 2836. (g) Lescouëzec, R.; Lloret, F.; Julve, M.; Vaissermann, J.; Verdaguer, M.; Llusar, R.; Uriel, S. *Inorg. Chem.* **2001**, *40*, 2065. (h) Wang, S.; Day, P.; Toma, L. M.; Julve, M.; Wallis, J. D. *Inorg. Chim. Acta* **2006**, *359*, 3283.
(17) (a) De Munno, G.; Bruno, G. *Acta Crystallogr.* **1984**, *C40*, 2030. (b) Julve, M.; De Munno, G.; Bruno, G.; Verdaguer, M. *Inorg. Chem.* **1988**, *27*, 3160. (c) Julve, M.; Verdaguer, M.; De Munno, G.; Real, J. A.; Bruno, G. *Inorg. Chem.* **1993**, *32*, 795. (d) De Munno, G.; Julve, M.; Nicolò, F.; Lloret, F.; Faus, J.; Ruiz, R.; Sinn, E. *Angew. Chem., Int. Ed. Engl.* **1993**, *32*, 613. (e) De Munno, G.; Julve, M.; Lloret, F.; Faus, J.; Verdaguer, M.; Caneschi, A. *Angew. Chem., Int. Ed. Engl.* **1993**, *32*, 1046. (f) De Munno, G.; Julve, M.; Lloret, F.; Derory, A. *J. Chem. Soc., Dalton Trans.* **1993**, 1179. (g) Andrés, E.; De Munno, G.; Julve, M.; Real, J. A.; Lloret, F. *J. Chem. Soc., Dalton Trans.* **1993**, 2169. (h) De Munno, G.; Julve, M.; Lloret, F.; Faus, J.; Caneschi, A. *J. Chem. Soc., Dalton Trans.* **1994**, 1175. (i) Castro, I.; Sletten, J.; Glærum, L. K.; Lloret, F.; Faus, J.; Julve, M. *J. Chem. Soc., Dalton Trans.* **1994**, 2777. (j) Castro, I.; Sletten, J.; Glærum, L. K.; Cano, J.; Lloret, F.; Faus, J.; Julve, M. *J. Chem. Soc., Dalton Trans.* **1995**, 3207. (k) De Munno, G.; Julve, M.; Lloret, F.; Faus, J.; Verdaguer, M.; Caneschi, A. *Inorg. Chem.* **1995**, *34*, 157. (l) De Munno, G.; Ruiz, R.; Lloret, F.; Faus, J.; Sessoli, R.; Julve, M. *Inorg. Chem.* **1995**, *34*, 408. (m) De Munno, G.; Julve, M.; Lloret, F.; Cano, J.; Caneschi, A. *Inorg. Chem.* **1995**, *34*, 2048. (n) De Munno, G.; Poerio, T.; Viau, G.; Julve, M.; Lloret, F.; Journaux, Y.; Rivière, E. *Chem. Commun.* **1996**, 2587. (o) De Munno, G.; Julve, M.; Viau, G.; Lloret, F.; Faus, J.; Viterbo, D. *Angew. Chem., Int. Ed. Engl.* **1996**, *35*, 1807. (p) De Munno, G.; Julve, M.; Real, J. A. *Inorg. Chim. Acta* **1997**, *255*, 185. (q) Sletten, J.; Daraghmeh, H.; Lloret, F.; Julve, M. *Inorg. Chim. Acta* **1998**, *279*, 127. (r) De Munno, G.; Armentano, D.; Julve, M.; Lloret, F.; Lescouëzec, R.; Faus, J. *Inorg. Chem.* **1999**, *38*, 2234. (s) Rodríguez-Martín, Y.; Sanchiz, J.; Ruiz-Pérez, C.; Lloret, F.; Julve, M. *Inorg. Chim. Acta* **2001**, *326*, 20. (t) Marinescu, G.; Lescouëzec, R.; Armentano, D.; De Munno, G.; Andruh, M.; Uriel, S.; Llusar, R.; Lloret, F.; Julve, M. *Inorg. Chim. Acta* **2002**, *336*, 46. (u) Armentano, D.; De Munno, G.; Lloret, F.; Julve, M.; Curély, J.; Babb, A. M.; Lu, J. Y. *New J. Chem.* **2003**, *27*, 161. (v) Herrera, J. M.; Armentano, D.; De Munno, G.; Lloret, F.; Julve, M.; Verdaguer, M. *New J. Chem.* **2003**, *27*, 128. (w) Marino, N.; Mastropietro, T. P.; Armentano, D.; De Munno, G.; Doyle, R. P.; Lloret, F.; Julve, M. *Dalton Trans.* **2008**, 5152. (x) Marino, N.; Armentano, D.; De Munno, G.; Cano, J.; Lloret, F.; Julve, M. *Inorg. Chem.* **2012**, *51*, 4323.
(18) (a) Real, A.; Zarembowitch, J.; Kahn, O.; Solans, X. *Inorg. Chem.* **1987**, *26*, 2939. (b) Gaspar, A. B.; Ksenofontov, V.; Martínez, V.; Muñoz, M. C.; Real, J. A.; Gütlich, P. *Eur. J. Inorg. Chem.* **2004**, 4770.
(19) (a) Cortés, R.; Lezama, L.; Pizarro, J. L.; Arriortua, M. I.; Rojo, T. *Angew. Chem., Int. Ed. Engl.* **1996**, *35*, 1810. (b) Cortés, R.; Urtiaga, M. K.; Lezama, L.; Pizarro, J. L.; Arriortua, M. I.; Rojo, T. *Inorg. Chem.* **1997**, *36*, 5016. (c) Martín, S.; Barandika, M. G.; Ruiz de Larramendi, J. I.; Cortés, R.; Font-Bardía, M.; Lezama, L.; Serna, Z. E.; Solans, X.; Rojo, T. *Inorg. Chem.* **2001**, *40*, 3687. (d) Martín, S.; Barandika, M. G.; Cortés, R.; Ruiz de Larramendi, J. I.; Urtiaga, M. K.; Lezama, L.; Arriortua, M. I.; Rojo, T. *Eur. J. Inorg. Chem.* **2001**, 2107.
(20) (a) Bérézovsky, F.; Hajem, A. A.; Triki, S.; Sala Pala, J.; Molinié, P. *Inorg. Chim. Acta* **1999**, *8*, 284. (b) Triki, S.; Thétiot, F.; Galán-Mascarós, J. R.; Sala Pala, J.; Dunbar, K. R. *New J. Chem.* **2001**, *25*, 954. (c) Thétiot, F.; Triki, S.; Sala Pala, J.; Galán-Mascarós, J. R.; Martínez-Agudo, J. M.; Dunbar, K. R. *Eur. J. Inorg. Chem.* **2004**, 3783. (d) Thétiot, F.; Triki, S.; Sala Pala, J.; Golhen, S. *Inorg. Chim. Acta* **2005**, *358*, 3277.
(21) Decurtins, S.; Schmalle, H. W.; Schneuwly, P.; Zheng, L.-M.; Ensling, J.; Hauser, A. *Inorg. Chem.* **1995**, *34*, 5501.
(22) Marshall, S. R.; Incarvito, C. D.; Manson, J. L.; Rheingold, A. L.; Miller, J. S. *Inorg. Chem.* **2000**, *39*, 1969.
(23) Kawata, S.; Kitagawa, S.; Enomoto, M.; Kumagai, H.; Katada, M. *Inorg. Chim. Acta* **1998**, *283*, 80.
(24) Colacio, E.; Lloret, F.; Navarrete, M.; Romerosa, A.; Stoeckli-Evans, H.; Suárez-Varela, J. *New J. Chem.* **2005**, *29*, 1189.
(25) Pointillart, F.; Herson, P.; Boubekeur, K.; Train, C. *Inorg. Chim. Acta* **2008**, *361*, 373.
(26) (a) Martínez, J.-L.; Armentano, D.; De Munno, G.; Cano, J.; Lloret, F.; Julve, M.; Faus, J. *Inorg. Chem.* **2011**, *50*, 12405. (b) Martínez, J.-L.; Lloret, F.; Julve, M.; Faus, J. *J. Coord. Chem.* **2009**, *62*, 92.
(27) Shavaleev, N. M.; Bell, Z. R.; Ward, M. D. *J. Chem. Soc., Dalton Trans.* **2002**, 3925.
(28) (a) Swavey, S.; Swavey, R. *Coord. Chem. Rev.* **2009**, *253*, 2627. (a) Fratini, A.; Richards, G.; Larder, E.; Swavey, S. *Inorg. Chem.* **2008**, *48*, 1030. (b) Richard, G.; Osterwyk, J.; Flikkema, J.; Cobb, K.; Sullivan, M.; Swavey, S. *Inorg. Chem. Commun.* **2008**, *11*, 1385. (c) Fratini, A.; Swavey, S. *Inorg. Chem. Commun.* **2007**, *10*, 636. (d) Swavey, S.; Krause, J. A.; Collins, D.; D'Cunha, D.; Fratini, A. *Polyhedron* **2008**, *27*, 1061. (e) Sultan, R.; Gadamsetti, K.; Swavey, S. *Inorg. Chim. Acta* **2006**, *359*, 1233.
(29) (a) Jang, H.; Shim Sultan, C. H.; Jung, B.-J.; Kim, D-h.; Shim, H.-K.; Do, Y. *Eur. J. Inorg. Chem.* **2006**, 718. (b) Fernandes, J. A.; Sá Ferreira, R.; Pillinger, M.; Carlos, L. D.; Jepsen, J.; Hazell, A.; Ribeiro-Claro, P.; Gonçalves, I. S. *J. Lumin.* **2005**, *113*, 50. (c) Bekiali, V.; Thiakou, K. A.; Ratpopoulou, C. P.; Perlepes, S. P.; Lianos, P. *J. Lumin.* **2008**, *128*, 481. (d) Baker, M. H.; Dorweiler, J. D.; Ley, A. N.; Pike, R. D.; Berry, S. M. *Polyhedron* **2009**, *28*, 188. (e) Znovjyak, K. O.; Moroz, O. V.; Ovchynnikov, V. A.; Sliva, T. Y.; Shishkina, S. V.; Amirkhanov, V. M. *Polyhedron* **2009**, *28*, 3731.
(30) (a) Ephritikhine, M.; Rivière, E.; Thuèry, P.; Zucchi, P. *Chem. Commun.* **2010**, *46*, 9143. (b) Zucchi, G.; Jeon, T.; Tondelier, D.; Aldakov, D.; Thuèry, P.; Ephritikhine, M.; Geffroy, B. *J. Mater. Chem.*

2010, *20*, 2114. (c) Zucchi, G.; Maury, O.; Thuèry, P.; Ephritikhine, M. *Inorg. Chem.* **2008**, *47*, 10398.
(31) Koziel, M.; Pelka, R.; Rams, M.; Nitek, W.; Sieklucka, B. *Inorg. Chem.* **2010**, *49*, 4268.
(32) Berg, D. J.; Boncella, J. M.; Andersen, R. A. *Organometallics* **2002**, *21*, 4622.
(33) Lazarides, T.; Adams, H.; Sykes, D.; Faulkner, S.; Calogero, G.; Ward, M. D. *Dalton Trans.* **2008**, 691.
(34) (a) Hooft, R. W. W. *COLLECT*; Nonius BV: Delft, The Netherlands, 1999; (b) Duisenberg, A. J. M.; Kroon-Batenburg, L. M. J.; Schreurs, A. M. M. *J. Appl. Crystallogr.* **2003**, *36*, 220 (EVALCCD).
(35) Spek, A. L. *J. Appl. Crystallogr.* **2003**, *36*, 7.
(36) Sheldrick, G. M. *Acta Crystallogr.* **2008**, *A64*, 112.
(37) Farrugia, L. J. *J. Appl. Crystallogr.* **1999**, *32*, 837.
(38) Nardelli, M. *J. Appl. Crystallogr.* **1995**, *28*, 659.
(39) *DIAMOND 2.1d, Crystal Impact GbR, CRYSTAL IMPACT*; K. Brandenburg & H. Putz GbR: Bonn, Germany, 2000.
(40) Ribas Gispert, J. *Coordination Chemistry*; Wiley-VCH: Weinheim, Germany, 2008; pp 77−78.